

IE

CERN LIBRARIES, GENEVA



CM-P00061042

Tracking studies on the beam-beam effect in the CERN-SPS $p \bar{p}$ collider

W.Herr, M.Meddahi, R.Schmidt
SL Division, CERN, Geneva, Switzerland

Abstract

During proton-antiproton runs in the SPS collider it has been observed that particles are lost on high order resonances. A simulation program has been developed to support experimental data and theoretical studies. With simple assumptions it was possible to qualitatively describe the particle losses on the 16th order resonance. Resonance trapping and stochastic behaviour have been identified as possible theoretical models to explain the tracking results and the observations.

Geneva, Switzerland

12 September 1991

Contents

1	Introduction	3
2	Description of the simulation program	4
3	Resonance island width in one dimension	4
3.1	Calculation of the resonance island width	4
3.2	Measurements of the resonance island width by tracking	6
3.2.1	Tune scans	6
3.2.2	Amplitude scan	7
3.2.3	Dependence of the island width on the linear beam-beam tune shift .	7
3.2.4	Phase space observations for different particle amplitudes	7
4	Tune modulation	9
4.1	Generalities	9
4.1.1	Synchrotron resonances	9
4.1.2	Expression for island width with tune modulation	10
4.1.3	Expression for the island separation	10
4.2	Tracking results and stochastic limit	10
4.2.1	Modulation frequency scan	10
4.2.2	Resonance trapping	11
4.2.3	Resonance overlap	12
4.2.4	Spectra from the modulation frequency scan	14
4.2.5	Modulation amplitude scan	14
4.3	Spectra from the modulation amplitude scan	15
5	Tracking results in two dimensions	16
6	Conclusion	17

1 Introduction

During the initial operation of the SPS $p\bar{p}$ collider the acceptable tune spread was limited to the available tunespace between resonances of order 3 and 10 for the working point of $Q_h = 26.7$ and $Q_v = 27.7$. A detrimental effect of resonances of higher order was not observed.

To achieve higher luminosities, the SPS collider was upgraded to operate with separated beams which allowed to inject 6 bunches per beam. As a consequence of the beam separation during the injection process the emittances of protons and antiprotons were conserved and resulted in unequal beam sizes since the initial antiproton emittances were smaller than for protons.

It was an unexpected observation that now higher order resonances, in particular the 16th order $16Q_x = 11$, became visible and limited the collider performance. In a series of dedicated experiments it was demonstrated that the strength of this resonance increases for beams with unequal emittances. An possible explanation for this observation was proposed in a recent paper [1].

For a better understanding of the mechanisms leading to particle losses in the presence of beam-beam interactions a simulation program was developed and the results obtained are discussed in this report.

Particle tracking is widely used to simulate the behaviour of particles in nonlinear fields and is an excellent tool for qualitative and quantitative studies of the beam-beam interaction.

In the first part of the report we shall compare the tracking results with theoretical predictions and therefore restrict the simulation to one plane. In particular, we shall measure the island width and study the effect of tune modulation on the particle stability. We show that, depending on the parameters, we observe stable islands, stochastic bands and the mechanism of resonance trapping.

In a further step we generalise the simulation for two transverse dimensions. Quantitative models for this case are not available. From the tracking we conclude that particle losses can occur for a much wider range of parameters than in the case of one dimension.

2 Description of the simulation program

We simulate the particle motion in a supposedly linear machine by a linear, uncoupled transformation and by a localised, non-linear beam-beam kick.

For a round Gaussian beam, the head-on beam-beam kicks are given as:

$$\delta x' = -\frac{8\pi\xi\sigma^2x}{r^2\beta}(1 - \exp(-\frac{r^2}{2\sigma^2})) \quad (1)$$

$$\delta y' = -\frac{8\pi\xi\sigma^2y}{r^2\beta}(1 - \exp(-\frac{r^2}{2\sigma^2})) \quad (2)$$

with $r^2 = x^2 + y^2$, ξ the linear beam-beam tune shift, σ the transverse dimension of the beam and β the betatron function at the interaction point. We assume round beams, e.g. $\sigma = \sigma_x = \sigma_y$. Transforming to new variables $\bar{x} = x/\sigma$ and $\bar{x}' = \beta \times x'/\sigma$, we get the position and the angle of a particle after turn $n+1$ from its coordinates after turn n by the non-linear map:

$$\bar{x}_{n+1} = \bar{x}_n \cos 2\pi Q_{xn} + \bar{x}'_n \sin 2\pi Q_{xn} \quad (3)$$

$$\bar{x}'_{n+1} = -\bar{x}_n \sin 2\pi Q_{xn} + \bar{x}'_n \cos 2\pi Q_{xn} + \delta\bar{x}'_{n+1} \quad (4)$$

$$\bar{y}_{n+1} = \bar{y}_n \cos 2\pi Q_{yn} + \bar{y}'_n \sin 2\pi Q_{yn} \quad (5)$$

$$\bar{y}'_{n+1} = -\bar{y}_n \sin 2\pi Q_{yn} + \bar{y}'_n \cos 2\pi Q_{yn} + \delta\bar{y}'_{n+1} \quad (6)$$

The simulation was performed for different initial particle amplitudes. The beams are colliding head-on and the linear beam-beam tune shift ξ is 0.005. This corresponds to typical values for the tune shifts per interaction point in the SPS ppbar collider. In order to place the particle onto the 16th order resonance the initial tune was chosen taking into account the detuning function which can be calculated:

$$Q_{init} = Q_{16^{th}} - \xi \times \Delta Q \quad (7)$$

with ΔQ the relative detuning for a certain particle amplitude. Another method which is more precise but very time consuming would be to perform a tune scan to get the initial tune needed to put a particle on the 16th order resonance.

As we will discuss later in more detail, the phase space trajectories depend on the initial parameters. For the particle motion in one transverse dimension three different types for the dynamical behaviour can be distinguished:

- the particle is trapped in an island.
- the particle is bound in a stochastic band.
- the particle amplitude increases until it is lost.

In the case of a particle trapped in an island in phase space, the island width can be measured and compared with analytical calculation.

3 Resonance island width in one dimension

3.1 Calculation of the resonance island width

In this section we study an isolated non linear resonance in the case of one degree of freedom using the Hamiltonian formalism. The theoretical model of single isolated resonances has

been known for a long time. Here, we follow the calculations by Ruth [2].

We assume that we are close to a resonance ($n \times Q = p$, where n is the resonance order and both n and p are integers). If we make the assumption that all other non resonant terms in the Hamiltonian can be neglected, the Hamiltonian becomes (in action-angle variables):

$$H = Q\alpha + \xi U(\alpha) + \xi V_n(\alpha) \cos(n\phi - p\theta) \quad (8)$$

with Q the tune, $U(\alpha)$ the primitive of the detuning function, $V_n(\alpha)$ the primitive of the resonance strength function for a resonance of order n , α the action coordinate, θ the angle which determines the position of the particle in the ring (i.e the independent or "time" variable) and ϕ the angle coordinate.

This problem can be solved exactly by a canonical transformation into a rotating system in phase space.

The generating function [3] for the transformation $(\alpha, \phi) \rightarrow (\alpha_1, \phi_1)$ is

$$F_2(\alpha_1, \phi) = (\phi - p\theta/n) \quad (9)$$

which yields the transformation equations:

$$\begin{aligned} \phi_1 &= \phi - p\theta/n \\ \alpha_1 &= \alpha \end{aligned} \quad (10)$$

The new Hamiltonian is then given by:

$$H_1(\phi_1, \alpha_1) = (Q - p/n)\alpha_1 + \xi U(\alpha_1) + \xi V_n(\alpha_1) \cos n\phi_1 \quad (11)$$

The Hamiltonian has been cast into a form explicitly independent of the 'time' variable θ ; therefore it is a constant of the motion.

In phase space (ϕ_1, α_1) we can find a set of points where the trajectories are stationary. The location of these *fixed points* are determined by solving the equation:

$$\frac{\partial H_1}{\partial \alpha_1} = \frac{\partial H_1}{\partial \phi_1} = 0$$

We get:

$$\sin n\phi_1 = 0 \quad (12)$$

$$(Q - p/n) + \xi U'(\alpha_1) + \xi V_n'(\alpha_1) \cos n\phi_1 = 0 \quad (13)$$

where the prime indicates differentiation with respect to α_1 . In action-angle variables (α_1, ϕ_1) , these form a sequence of points surrounding the origin (Fig.1 taken from [2]). The fixed points are stable for $\cos n\phi_1 = -1$ and unstable for $\cos n\phi_1 = +1$ corresponding to a minimum or a maximum of the potential. If α_u is the amplitude which gives an oscillation frequency at resonance

$$Q + U'(\alpha_u) = p/n \quad (14)$$

equation (13) becomes :

$$U'(\alpha_1) - U'(\alpha_u) + V_n'(\alpha_1) \cos n\phi_1 = 0 \quad (15)$$

or expanding α_1 close to α_u

$$(\alpha_1 - \alpha_u) = \frac{V'(\alpha_u)}{U''(\alpha_u)} \cos n\phi_1 \quad (16)$$

The boundaries of the stable islands are defined by the separatrix which are the largest closed curve surrounded the stable fixed point. Their equation can be easily found by the fact that the new Hamiltonian H_1 is a constant.

From equations (11) and (13) we get:

$$(Q - p/n)\alpha_1 + \xi U(\alpha_1) - \xi V_n(\alpha_1) = (Q - p/n)\alpha_u + \xi U(\alpha_u) + \xi V_n(\alpha_u) \quad (17)$$

where α_u is the action at the unstable fixed point. Expanding α close to α_u and recalling that $\alpha_r \simeq \alpha_u$, we find that on the separatrix:

$$(\alpha - \alpha_u)^2 \simeq \frac{4V(\alpha_u)}{U''(\alpha_u)} \quad (18)$$

From this equation we find the maximum separation or island width:

$$\alpha_r = 4\sqrt{\frac{V(\alpha_r)}{U''(\alpha_r)}} \quad (19)$$

where $U''(\alpha_r)$ has been assumed positive for simplicity. This equation is only valid when $\alpha_r \ll \alpha_u$. In addition, other resonances which have so far been neglected must be far away. If neighboring resonances overlap each other, then it is clearly incorrect to calculate the island width assuming isolated resonances.

We have already calculated the expression for the detuning function and the resonance strength function in another report [4] :

$$U'(\alpha) = \frac{2}{\alpha} [1 - \exp(-\frac{\alpha}{2}) \times I_0(\frac{\alpha}{2})] \quad (20)$$

$$V'_n(\alpha) = (-1)^{\frac{n}{2}+1} \frac{4}{\alpha} \exp(-\frac{\alpha}{2}) \times I_n(\frac{\alpha}{2}) \quad (21)$$

where I_0 is the modified Bessel function of order zero.

By taking the derivative of equation (20) and integrating equation (21) we obtain the expression for the island half-width and can plot it as a function of the particle amplitude (Fig.2). To summarize the phase space plot shown in Fig.1, at small amplitudes the motion is relatively unaffected by the resonance and the particle moves along a circle. Near the resonance the circles are distorted. Finally, at the resonant amplitude there is a string of stable islands with widths determined (approximatively) by equation (19).

3.2 Measurements of the resonance island width by tracking

3.2.1 TUNE SCANS

For one particle tune, we run the tracking program and get the maximum particle amplitude (ϵ_{max}) after 2^{18} turns. We change the particle tune and obtain the new maximum value of

the particle amplitude for the same number of turns, and so on [5].

After performing this tune scan, we plot the ratio $\epsilon_{max}/\epsilon_{min}$ as a function of the initial tune. The resulting plot shows two peaks which correspond to the two particle positions in the phase space where the particle reaches its maximum amplitude. The distance between the two peaks corresponds to the resonance island width in units of tune (Fig.4a, to be compared to Fig.3 extracted from [6]). The peak in the tune spectrum is not at the position of the initial tune but at $Q_{init} + \xi \times \Delta Q$ due to the beam-beam detuning [e.g.(7)].

3.2.2 AMPLITUDE SCAN

For a fixed tune, we perform an amplitude scan and plot the difference between the starting tune and the tune corresponding to the main peak as a function of the demanded particle amplitude. We notice that in a certain range of amplitudes this detuning is constant: the particle is trapped inside the island. This range of amplitudes gives the resonance island width in units of sigma of the particle (Fig.4b).

3.2.3 DEPENDENCE OF THE ISLAND WIDTH ON THE LINEAR BEAM-BEAM TUNE SHIFT

From equation (19) it is clear that the resonance width is independent of the linear beam-beam tune shift, as long as the resonance condition at the amplitude α is satisfied. This property is well reproduced by computer tracking, as can be seen below: for a particle with a starting amplitude of 5σ , the resonance width obtained is $\Delta Q_r = 5 \times 10^{-5}$ for all the different values of ξ considered.

ξ	ΔQ_r
0.001	5×10^{-5}
0.005	5×10^{-5}
0.01	5×10^{-5}

3.2.4 PHASE SPACE OBSERVATIONS FOR DIFFERENT PARTICLE AMPLITUDES

For a fixed particle amplitude, we follow the particle motion in phase space as we change the initial tune ($\Delta Q_{step} = 3 \times 10^{-8}$).

The particle motion in phase space is a closed trajectory and the particle amplitude is increasing or decreasing depending on the instantaneous tune. The phase space observation is done in Fig.5 for a particle amplitude of 6σ . Starting close to the separatrix (Fig.5a,5b), as we increase slowly the starting tune, we observe that the area enclosed by the trajectory shrinks (Fig.5c,5d) until the fixed point is reached. Then, increasing the tune further, causes the enclosed area to grow until the trajectory again comes close to the separatrix (Fig.5e,5f). We summarize in the following table the values for the island widths. They are expressed in units of tune (ΔQ_r) and are compared with theoretical predictions.

Particle amplitude	ΔQ_r tracking	ΔQ_r theory
5σ	5×10^{-5}	3.1×10^{-5}
6σ	8×10^{-5}	7.1×10^{-5}
8σ	1.11×10^{-4}	1.32×10^{-4}
10σ	1.1×10^{-4}	1.4×10^{-4}
12σ	1×10^{-4}	1.21×10^{-4}

The island widths are also expressed in units of σ ($\Delta\alpha_r$) and are compared with theoretical predictions:

<i>Particle amplitude</i>	$\Delta\alpha_r$ <i>tracking</i>	$\Delta\alpha_r$ <i>theory</i>
5σ	0.3	0.252
6σ	0.5	0.614

The calculated value for the width gives just an idea of the exact value: formula (19) gives the width of the resonance by doubling the half width and from the phase space plot is it easy to realise that the definition of the half width is an approximation: the islands are not symmetric. Therefore, the theoretical value is just an approximate value of the width and we can say that there is a good agreement between the measured and the calculated width.

We also make the comparison between theory and tracking for the 10^{th} order resonance and find a good agreement:

<i>Tracking</i>		<i>Theory</i>	
ΔQ_r	$\Delta\alpha_r$	ΔQ_r	$\Delta\alpha_r$
9.19×10^{-5}	0.5	7.06×10^{-5}	0.5

4 Tune modulation

4.1 Generalities

4.1.1 SYNCHROBETATRON RESONANCES

Tune modulation can result from several mechanisms: one source is a small ripple on the quadrupole power supplies. A natural source is the tune variation accompanying energy oscillations when the chromaticity is not zero. In this case the modulation frequency is the synchrotron frequency, which is up to 180 Hz in the SPS.

This tune modulation will cause the particles to continually sweep across resonances and one should expect that the phase space trajectories are affected.

We assume that due to an external modulating source, the unperturbed betatron tune is given by:

$$Q = Q_0 + \hat{Q} \sin(2\pi Q_{mod}t) \quad (22)$$

The Hamiltonian becomes [7]:

$$H_2 = (Q_0 + \hat{Q} \sin(2\pi Q_{mod}t) - p/n)\alpha_2 + \xi U(\alpha_2) + \xi V_n(\alpha_2) \cos n\phi_2 \quad (23)$$

After a canonical transformation where the new variables are given by (with k an integer):

$$\alpha_3 = \alpha_2 \quad (24)$$

$$\phi_3 = \phi_2 + \left(\frac{\hat{Q}}{Q_{mod}}\right) \cos(2\pi Q_{mod}t - 2\pi Q_{mod}kt/n) \quad (25)$$

the new Hamiltonian becomes:

$$H_3 = (Q_0 - p/n - Q_{mod}k/n)\alpha_3 + \xi U(\alpha_3) + \xi V_n(\alpha_3) \cos[n\phi - 2\pi Q_{mod}kt + \frac{n\hat{Q}}{Q_{mod}} \cos(2\pi Q_{mod}t)] \quad (26)$$

The final term can be expanded as a series of synchrobetatron side bands with spacing Q_{mod}/n , the coefficients being Bessel functions $J_k(\hat{Q}n/Q_{mod})$. Each of these terms can be treated as an independent resonance provided that the perturbation strength is weak enough that they do not overlap. We analyse them separately, choosing the appropriate value of k for each. We use the Hamiltonian H_k to estimate the width of the k^{th} side band. For qualitative discussion then, the Bessel function $J_k(K)$ can be approximated by zero when $K < k$ and by $(\pi K)^{-1/2}$ otherwise. We obtain for $k < k_{max} \equiv n \hat{Q}/Q_{mod}$:

$$H_k = (Q_0 - p/n - Q_{mod}k/n)\alpha + \xi U(\alpha) + \xi V_n(\alpha) \cos n\phi \sqrt{\frac{Q_{mod}}{\pi n \hat{Q}}} \quad (27)$$

As k has been fixed, the Hamiltonian is independent of time. In the range $\pm \hat{Q}$, about $2k_{max}$ lines have a significant strength.

For small Q_{mod} these sidebands are very close together and can give rise to resonance overlap and stochastic behaviour, as we will show in the next section.

4.1.2 EXPRESSION FOR ISLAND WIDTH WITH TUNE MODULATION

From equation (19) and remembering that the k^{th} sideband is weakened by a factor $J_k(\hat{Q}n/Q_{mod})$, the width of the island in α is:

$$\alpha_r = 4\sqrt{\frac{V_n(\alpha)}{U''(\alpha)}}J_k(\hat{Q}n/Q_{mod}) \quad (28)$$

For a large argument of the Bessel function,

$$J_k(\hat{Q}n/Q_{mod}) = \sqrt{\frac{Q_{mod}}{\pi n\hat{Q}}} \quad (29)$$

We finally get for the resonance width:

$$\alpha_r = 4\sqrt{\frac{V_n(\alpha)}{U''(\alpha)}}\left(\frac{Q_{mod}}{\pi n\hat{Q}}\right)^{1/4} \quad (30)$$

4.1.3 EXPRESSION FOR THE ISLAND SEPARATION

The separation in tune is:

$$Q_{separation} = \frac{Q_{mod}}{n} = \xi U''(\alpha)\alpha_{separation}$$

$$\alpha_{separation} = \frac{Q_{mod}}{n\xi U''(\alpha)} \quad (31)$$

4.2 Tracking results and stochastic limit

In the following, a particle at an amplitude of 5σ is studied. The fractional part of the initial tune is fixed at .68683. Taking into account the detuning at an amplitude of 5σ this value is required to place the particle onto 16th order resonances.

4.2.1 MODULATION FREQUENCY SCAN

As the tune modulation is switched on, the phase space coordinates of a particle have to be plotted once per modulation period [8]. Otherwise, the trajectories previously observed without modulation seem to have broken up into diffuse sidebands. However, if the phase space is strobed with the modulation period no 'stochastic' behaviour is seen: we observe an island structure of order 16.

In the following table, we have summarized the maximum particle amplitude during 2000000 turns for different values of the modulation frequency. The modulation frequency is varied from 0 up to the revolution frequency. The modulation amplitude is fixed at 0.002. The results are discussed in the following section.

Q_{mod}	<i>Modulation frequency in Hz</i>	<i>maximum amplitude</i>	<i>islands observed: Y/N</i>
0	0	5.01	Y
5×10^{-9}	8.67×10^{-6}	5.38	N
1×10^{-8}	4.3×10^{-4}	5.7	N
1×10^{-7}	0.0043	73.7	N
1×10^{-6}	0.043	45.5	N
1.6×10^{-6}	0.0694	48.1	N
1×10^{-5}	0.43	35.8	N
2×10^{-5}	0.867	5.54	N
2.5×10^{-5}	1.08	5.68	N
0.00005	2.16	5.88	N
0.0001	4.3	5.06	N
0.000125	5.42	5.01	Y
0.00014	6.19	5.077	N
0.00016	7.2	5.7	N
0.0002	8.67	6.2	N
0.00025	10.84	5.01	N
0.00033	14.45	5.016	N
0.0005	21.68	5.079	N
0.00066	28.91	5.075	Y
0.001	43.37	5.071	Y
0.00111	48.19	5.07	Y
0.00125	54.21	5.07	Y
0.00142	61.96	5.07	Y
0.00166	72.29	5.069	Y
0.002	86.75	5.069	Y
0.005	216	5.069	Y
0.02	867.5	5.122	Y
0.03333	1445.8	5.127	Y
0.1	4337.5	5	Y
1	43375	5	Y

At zero frequency the particle is trapped in the 16 islands (Fig.6a shows a zoom onto one of those islands). The phase space is stable. As we increase slightly the modulation frequency to 0.00043 Hz the particle amplitude starts to increase slowly but the phase space remains stable. As the frequency reaches the value of 0.0043 Hz the particle amplitudes increases immediately to a very large value (73σ). This enormous amplitude growth is still present until the modulation frequency reaches 0.867 Hz. At this frequency, the particle amplitude stabilizes itself around 5.3σ but no island structure is observed (Fig.6b). At 5.42 Hz, 16 islands are again present in the phase space (Fig.6c). From 28.91 Hz, island structures are always observed (Fig.6d, 6e, 6f, 6g).

4.2.2 RESONANCE TRAPPING

The enormous amplitude growth reached by the particle in the frequency range from 0.0043 Hz to 0.43 Hz can be explained by the phenomenon of resonance trapping. To explain this phenomenon, considerations of adiabaticity are useful: if a particle moves around a

fundamental resonance island many times in the time it takes for the island to be displaced by its width due to the tune modulation, the particle can be expected to remain trapped and to move with the island.

Particles initially captured in stable islands at small amplitudes will move with the island to larger amplitudes as long as the adiabaticity condition is satisfied. This mechanism is closely analogous to the process of adiabatic capture and stacking in synchrotron phase space and it forms the basis of the resonance trapping model of Month [9]. Obviously as the tune modulation direction reverses, the islands contract and retrace their original paths finally transporting the particles back to their starting points. However, if in the course of the movement the island amplitude exceeds the aperture of the machine or if the adiabaticity condition is violated particle loss can result.

Expressing this condition quantitatively gives a critical frequency Q_c below which resonance trapping occurs [10];

$$Q_c = n\xi^2 \frac{V_n(\alpha_n)U''(\alpha_n)}{\hat{Q}} \quad (32)$$

x/σ	Q_c	$f_c(Hz)$
2σ	0.57×10^{-9}	2.47×10^{-5}
3σ	0.53×10^{-7}	2.29×10^{-3}
4σ	0.59×10^{-6}	0.025
5σ	0.22×10^{-5}	0.095

The above table shows that for the resonance of order 16 the critical capture frequency is more than a few orders of magnitude lower than the synchrotron frequency (178 Hz) so this process cannot be driven by energy oscillations.

However the critical frequency falls in a range where power supply ripple can become important and it has been observed experimentally that the antiproton lifetime is very sensitive to low frequency power supply ripple.

This diffusion process is very fast : the particle is lost before one turn of the modulation is finished. The particle amplitude is then very sensitive to the modulation phase. If we change the modulation phase ($Q = Q_0 - \hat{Q} \sin(2\pi Q_{mod}t)$) the particle amplitude remains very stable and stabilises itself at 5.08σ . If we also change the modulation phase for the other values of the modulation where the particle amplitude was increasing considerably, the same observation is made: the particle amplitude remains stable as it can be seen in the following table.

Q_{mod}	<i>Modulation frequency in Hz</i>	<i>maximum amplitude</i>
1×10^{-7}	0.0043	5.08
1×10^{-6}	0.043	5.06
1.6×10^{-6}	0.0694	5.08
1×10^{-5}	0.43	5.68

4.2.3 RESONANCE OVERLAP

Between 0.867 Hz and 4.3 Hz, the particle amplitude is stabilizing itself around 5.3σ and the phase space shows a stochastic band where the particle is trapped. This modest particle

amplitude growth is due to the phenomenon of resonance overlap. We have seen that tune modulation can lead to unstable or 'stochastic' behaviour. A stochastic behaviour is observed when the separatrices of different resonances touch each other. There exists a very well known criterion for the onset of stochasticity called the Chirikov criterion which states that the phase space becomes unstable when the resonance widths exceed their separation [11]. The effect of tune modulation is then to enormously increase the density of satellites and thereby reduce the Chirikov threshold.

To avoid stochastic behaviour, the island widths have to be smaller than the island spacing. For two resonances of half width $\Delta\alpha_{r1}$ and $\Delta\alpha_{r2}$ the Chirikov Criterion is:

$$\Delta\alpha_{r1} + \Delta\alpha_{r2} \ll \Delta\alpha_{island.sep} \quad (33)$$

For $\Delta\alpha_{r1} \simeq \Delta\alpha_{r2}$, we get:

$$\Delta\alpha_r \ll \Delta\alpha_{island.sep} \quad (34)$$

We apply this theory to explain the amplitude growth noticed in the modulation frequency scan when we approach 4.3 Hz.

We have summarized the value of the island width and the island separation for each value of the modulation frequency in the following table:

Q_{mod}	<i>Modulation frequency in Hz</i>	<i>Resonance width</i>	<i>Resonance separation</i>
1.45×10^{-5}	0.619	0.0063	0.0039
1.66×10^{-5}	0.722	0.0065	0.0045
2×10^{-5}	0.867	0.0068	0.0054
2.5×10^{-5}	1.084	0.0072	0.0068
3.33×10^{-5}	1.445	0.0078	0.0091
5×10^{-5}	2.168	0.0086	0.0136
1×10^{-4}	4.337	0.0103	0.0273
1.11×10^{-4}	4.819	0.0105	0.0303
1.25×10^{-4}	5.421	0.0108	0.0341
1.428×10^{-4}	6.196	0.0112	0.0390
1.666×10^{-4}	7.229	0.0117	0.0455
2×10^{-4}	8.675	0.0122	0.0546
2.5×10^{-4}	10.84	0.0129	0.0683
3.33×10^{-4}	14.45	0.0139	0.0911
5×10^{-4}	21.68	0.0154	0.1367
6.66×10^{-4}	28.91	0.0165	0.1823
2×10^{-3}	86.75	0.0217	0.5469
5×10^{-3}	216.8	0.0273	1.3674
2×10^{-2}	867.5	0.0387	5.4699

From a modulation frequency of 867 Hz down to 216 Hz, the island width is smaller than the island separation. The phase space shows islands as it was previously observed. When we decrease the modulation frequency, the resonance separation is continuously decreasing and as both the resonance separation and the resonance width get closer to each other a stochastic band is observed instead of the islands. For a frequency less than 1.445 Hz, the islands have overlapped (resonance width > resonance separation) and the particle amplitudes increase to very large values.

As we have seen, stochastic and regular trajectories can usually be distinguished visually in a phase space plot by whether or not they appear on a continuous curve. A more quantitative distinction occurs in the Fourier spectra of the trajectory.

4.2.4 SPECTRA FROM THE MODULATION FREQUENCY SCAN

We analyse five cases for which a modulation amplitude scan was done when the modulation amplitude was fixed at 0.002.

For a modulation frequency of 867 Hz (Fig.7), three peaks appear in the tune spectrum which correspond to the 16th order resonance and the two side bands of the first order satellite.

For a modulation frequency of 86.75 Hz (Fig.8), the tune spectrum shows four peaks corresponding to the modulation side bands of order 1 and 2 and one peak associated with the 16th order resonance.

For a modulation frequency of 43.375 Hz (Fig.9), the tune spectrum shows six peaks corresponding to the modulation side bands of order 1,2 and 3 and a peak at the 16th order resonance.

For a modulation frequency of 5.42 Hz (Fig.10), the number of peaks have been increased. But now a modulation frequency of 5.42 Hz gives a side band separation of 7.8×10^{-6} (Q_{mod}/n) and they are too closed to be seen separately.

At very low modulation frequency (< 0.5 Hz), the particle amplitude increases to very large values and the particle is lost.

For a modulation frequency of few Hz, (0.5 - 5 Hz) the phase space shows a stochastic band where the particle is trapped. This leads to a small increase of the particle amplitude but then the amplitude remains stable around 5.3σ . This particle amplitude growth depends strongly on the modulation amplitude as we will see in the following section.

4.2.5 MODULATION AMPLITUDE SCAN

The modulation frequency is fixed to 5.42 Hz and the amplitude is varying from 0 to 0.006. The maximum amplitude reached during 10 millions turns is shown and the phase space coordinates of the particle have been plotted once per modulation period.

<i>modulation amplitude</i>	<i>maximum amplitude</i>	<i>islands observed:Y/N</i>
0.000001	5.09	Y
0.00001	5.17	Y
0.0001	5.8	N
0.0005	14.09	N
0.001	35.75	N
0.0015	5.78	N
0.0018	10.85	N
0.0019	5.06	N
0.00195	24.79	N
0.001977	25.59	N
0.00198	5.015	Y
0.002	5.012	Y
0.005	5.014	Y
0.006	5.01	Y

From 0 to 0.00001 modulation amplitude, the phase space is stable and 16 islands are observed. Fig.11a shows one of the 16 islands for 1×10^{-5} modulation amplitude as we plot the phase space once per modulation period. If it is not done in such a way, the trajectories are no longer closed: with tune modulation, we introduce another dimension and the phase space symmetry is broken (Fig.11b).

Then, from 0.00001 to 0.001977 amplitude modulation, the particle amplitude performs dramatic and irregular fluctuations which are often much larger than a few σ (Fig.11c,11d,11e). The corresponding resonance width and resonance separation are summarized in the following table:

<i>modulation amplitude</i>	<i>resonance width</i>	<i>resonance separation</i>
0.0001	0.0230	0.0314
0.0005	0.015	0.0314
0.001	0.0129	0.0314
0.0015	0.0117	0.0314
0.0018	0.011	0.0314
0.0019	0.0110	0.0314
0.00195	0.01096	0.0314
0.001977	0.01092	0.0314
0.00198	0.01091	0.0314
0.002	0.01089	0.0314
0.005	0.00866	0.0314
0.006	0.00827	0.0314

As we increase the amplitude of the modulation, the ratio between the resonance width and the resonance separation decreases and in phase space islands are finally observed from 0.00198 to larger values (Fig.11f). For some modulation amplitudes (0.005,0.001, 0.00195, 0.001977), the particle amplitude reaches very large values. This process is not very fast: after 2 millions turns, the particle amplitudes is still around 5 to 6 σ . And if we change the modulation phase it is still increasing slowly. The regime is stochastic.

4.3 Spectra from the modulation amplitude scan

The modulation frequency is still fixed to 5.42 Hz.

At an amplitude of 0.00001, we have seen that the particle amplitude is stable (16 islands are present in the phase space). The tune spectrum shows one peak at the 16th order resonance (Fig.12).

As we increase the modulation amplitude to 0.001, the particle amplitude starts to increase and in the tunes pectrum we notice an increasing number of peaks. They are shown in a range defined by the quantity $\pm\hat{Q}$ (Fig.13) but as they are spaced by Q_{mod}/n they are too close to be seen separately.

At 0.00198, where the particle amplitude becomes again stable the tune spectrum shows more peaks than before but there is no more peak at the 16th order resonance (Fig.14).

If the modulation frequency is now fixed to 86.75 Hz, the tune spectrum for a modulation amplitude of 0.00001 shows one peak at the 16th order resonance (Fig.15).

For a modulation amplitude of 0.001, side bands of order 1 and 2 are identified (Fig.16) and for a modulation amplitude of 0.003, side bands of order 1,2 and 3 can be seen (Fig.17).

5 Tracking results in two dimensions

To study the effects of coupling between the two transverse planes on particle losses, the vertical dimension was added to the tracking program.

In the following table, we have summarized the maximum particle amplitudes reached after 2 and 8 million turns. The initial vertical oscillation amplitude was fixed at 5σ and 8σ . The modulation tune was varying from $2 \cdot 10^{-5}$ to 0.0001 and the amplitude of the modulation was fixed at 0.002.

$Amax_1$ and $Amax_2$ are the maximum particle amplitudes in one and two dimensions respectively.

For two dimensions, the tunes were ($Q_x = 26.6890$, $Q_y = 27.6864$) (Fig.18). For one dimension, the tune is exactly on the 16^{th} order resonance.

Q_{mod}	$Amax1$	$Amax2 (y = 5\sigma)$		$Amax2 (y = 8\sigma)$	
number of turns	$2 \cdot 10^6$	$2 \cdot 10^6$	$8 \cdot 10^6$	$2 \cdot 10^6$	$8 \cdot 10^6$
2×10^{-5}	5.54	7.65	17.53	25.75	25.79
2.5×10^{-5}	5.68	7.55	15.11	8.82	28.83
0.00005	5.88	8.78	16.37	11.07	19.16
0.0001	5.06	9.01	13.34	13.25	19.20

The addition of the second dimension leads to a strong increase of the particle amplitude. This increase is very strong if the tunes of the particle are placed in a region where coupling resonances are important.

If the particle has larger and larger oscillation amplitudes, it will cross more and more resonances. Then, diffusion is clearly observed and the particle is lost rapidly.

If we change the tunes of the particle and place them at ($Q_x = 0.6891$, $Q_y = 0.6803$) (Fig.18) the particle will cross less coupling resonances.

Q_{mod}	$Amax1$	$Amax2 (y = 5\sigma)$		$Amax2 (y = 8\sigma)$	
number of turns	$2 \cdot 10^6$	$2 \cdot 10^6$	$8 \cdot 10^6$	$2 \cdot 10^6$	$8 \cdot 10^6$
2×10^{-5}	5.54	5.30	6.19	7.95	14.37
2.5×10^{-5}	5.68	5.58	6.98	4.48	8.93
0.00005	5.88	5.96	10.32	5.98	6.26
0.0001	5.06	5.16	5.17	5.30	5.47

We observe that its amplitude increases very slowly, except for some values where the particle moves towards very large amplitudes.

By adding the second dimension, we introduce more resonances in the tune diagram and have more opportunities to get resonance overlap. The phase space is four dimensional and the stochastic bands observed in one dimension are not circles any more and communication can be established between them: the particle can move to larger and larger amplitudes.

6 Conclusion

During this tracking study, the particles losses were analysed near the 16th order resonances to explain the observed losses during the SPS operation. Two phenomena are present: for very low modulation frequencies (< 0.5 Hz) resonance trapping leads to very large values of the particle amplitude and the particles are finally lost. For frequencies of a few Hz, the particle is trapped in a stochastic band and a maximum amplitude is not exceeded. The increase of the particle amplitude depends strongly on the amplitude of the modulation. For a modulation of > 0.002 islands are observed in phase space. In two dimensions, both phenomena of resonance trapping and resonance overlap lead to particle losses.

References

- [1] K.Cornelis, M.Meddahi, R.Schmidt; *Experiments on the beam-beam effect in the CERN-SPS in the 1989 collider run*; SPS/AMS/Note 89-13.
- [2] R.Ruth; *Single particle dynamics in circular accelerator*; AIP Conference Proceedings 153 ; volume one, Slac summer school, 1985, Fermilab summer school, 1984.
- [3] H.Goldstein *Classical Mechanics*.
- [4] M.Meddahi and R.Schmidt; *Calculation of the tune spread induced by beam-beam effects in the case of partially separated beams*; CERN SL/90-15 (AP).
- [5] W.Herr; *Computer simulation of synchrotron resonances induced by a non-zero crossing angle in the LHC*; CERN SL/90-69 (AP).
- [6] A.L. Gerasimov, F.M. Izrailev and J.L. Tennyson; *Synchrotron sideband overlap in electron-positron colliding beams*; AIP Conference Proceedings 153 ; volume one, Slac summer school, 1985, Fermilab summer school, 1984.
- [7] S.Peggs; *Hadron collider behavior in the non-linear numerical model EVOL*; CERN/SPS 84-20 (DI-MST).
- [8] L.R.Evans; *The beam-beam interaction*; CERN SPS/83-38 (DI).
- [9] M.Month; *IEEE Trans. Nucl. Sci.* NS-22; 1276-80 (1975).
- [10] S.G.Peggs and R.M.Talman; *Nonlinear problems in accelerator physics*; Ann.Rev.Nucl.Part.Sci.1986.36:287-325.
- [11] B.Chirikov; *Physics Reports*; 52; p.263; (1979).

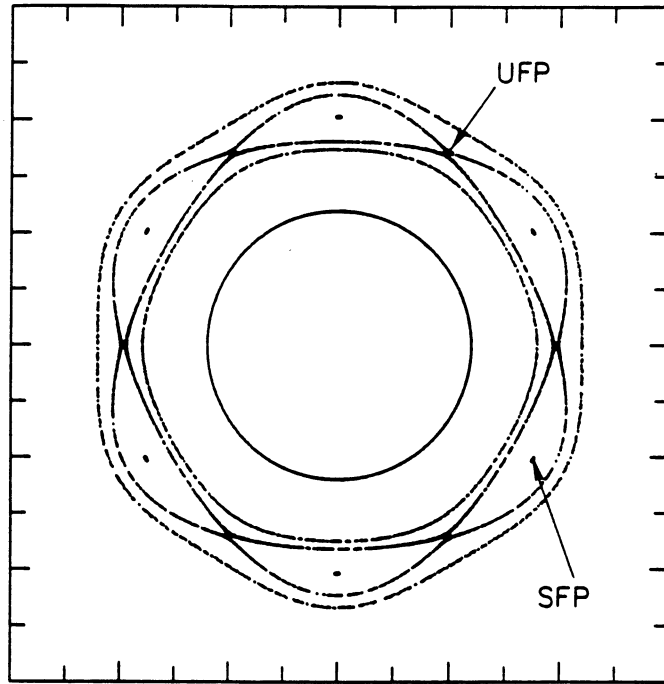


Fig.1: phase space for a sixth-order resonance.

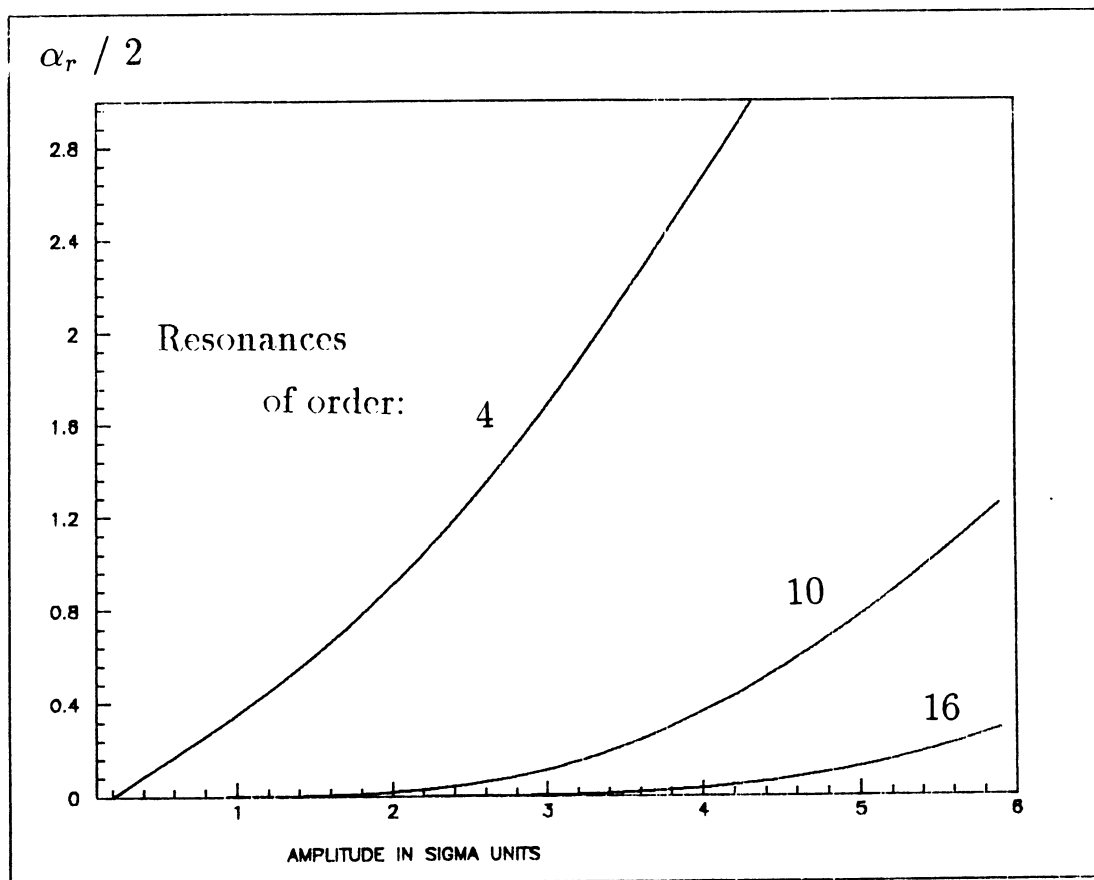


Fig.2: half island width as a function of the particle amplitude.

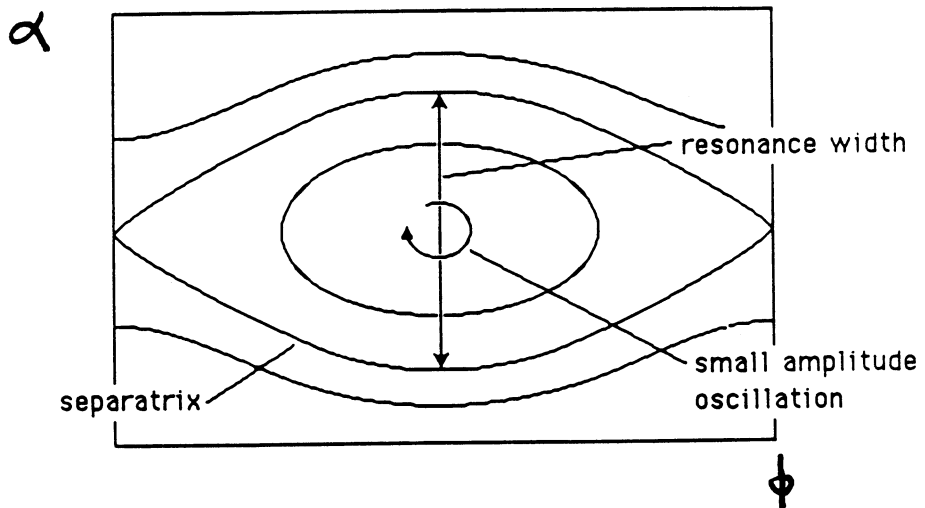


Fig.3: representation of an island width.

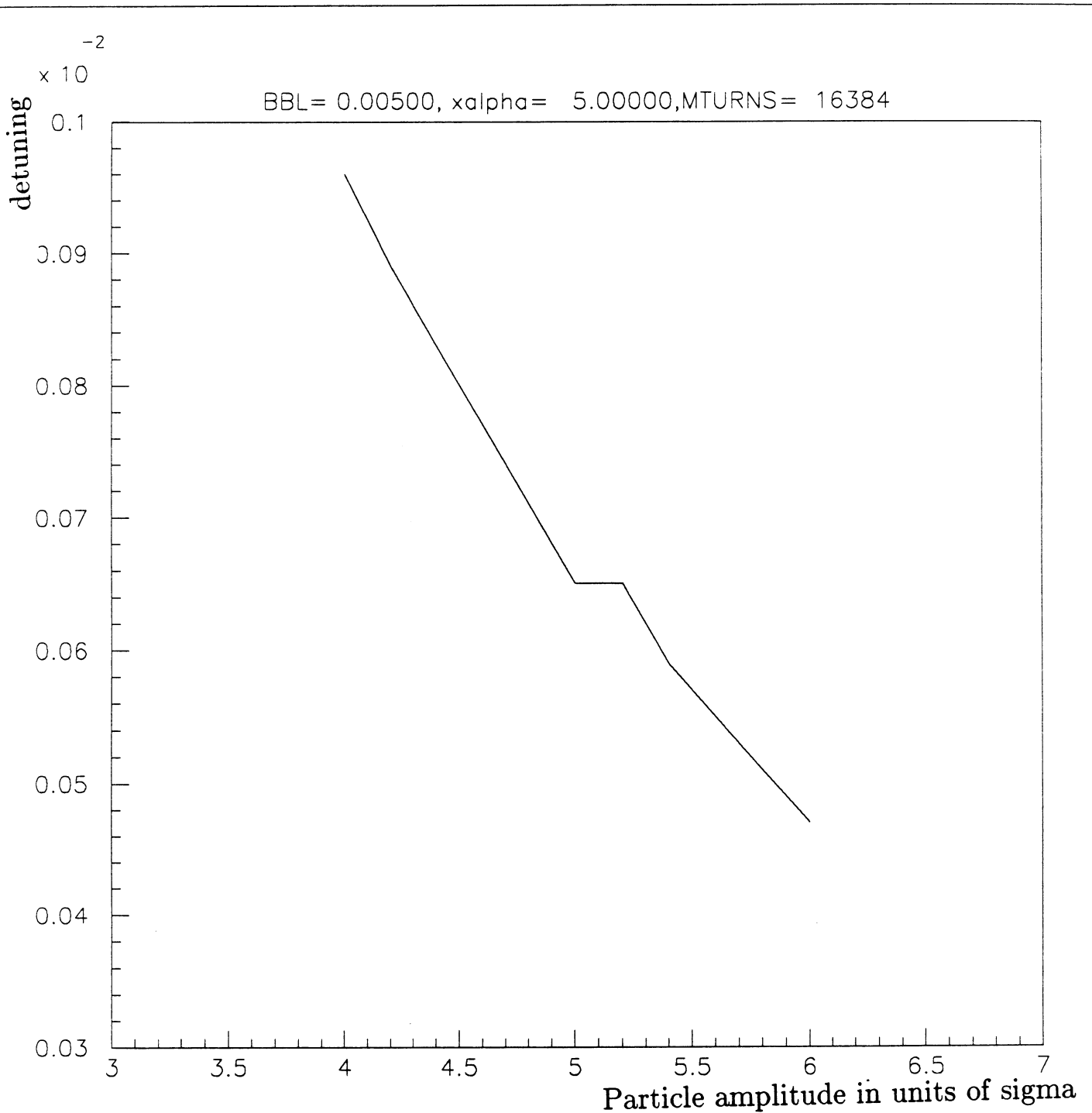


Fig.4b: detuning as a function of the particle amplitude.

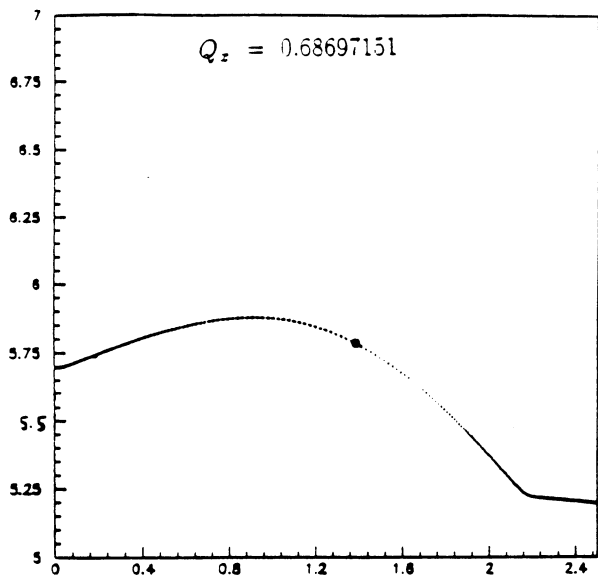


Fig.5a

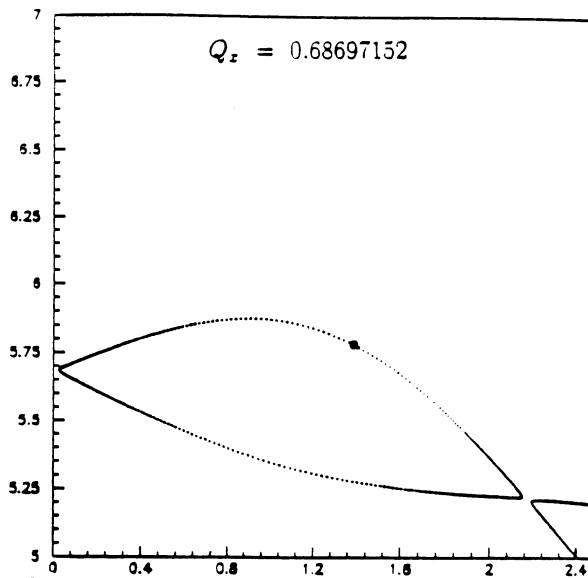


Fig.5b

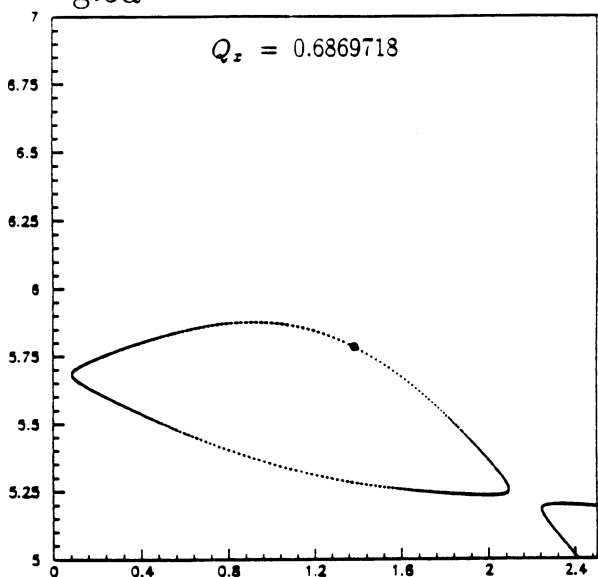


Fig.5c

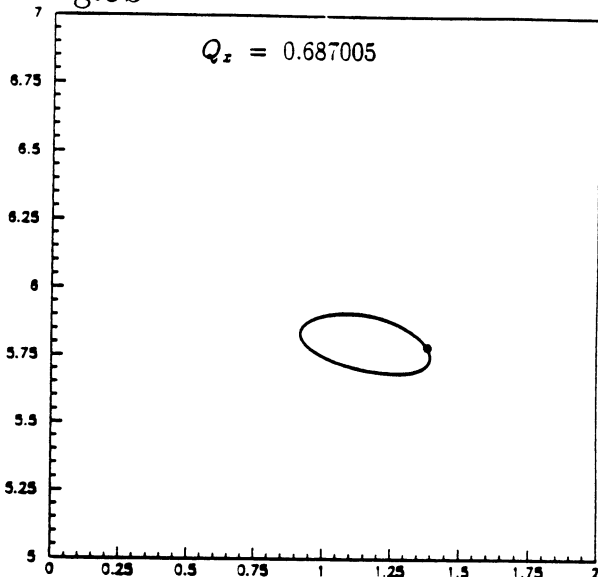


Fig.5d

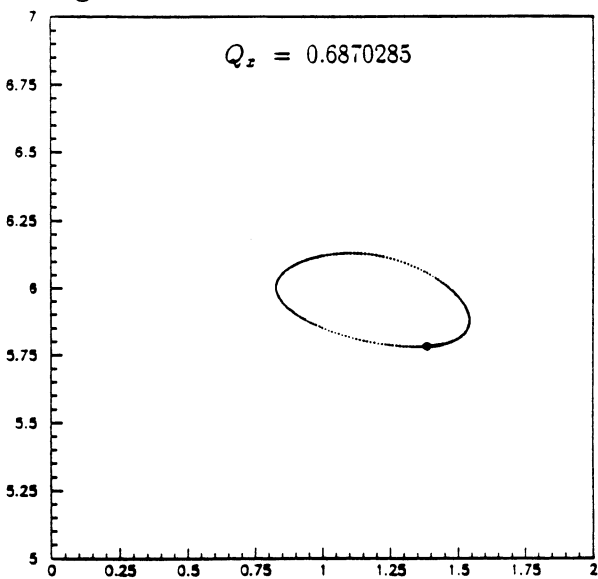


Fig.5e

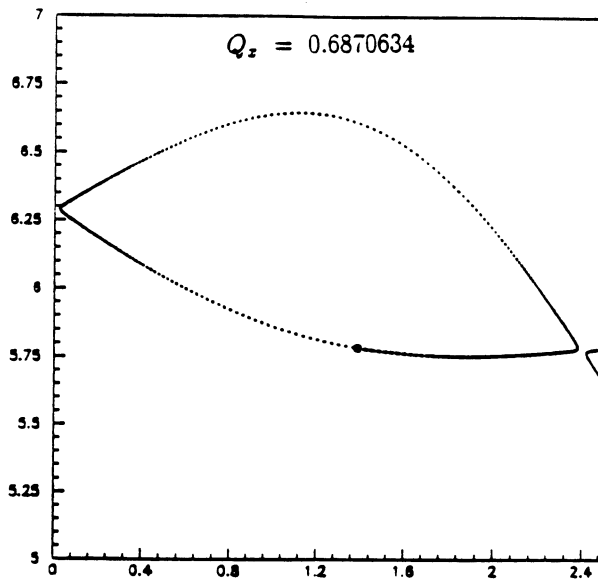


Fig.5f

Fig.5: phase space observations for different particle tunes.

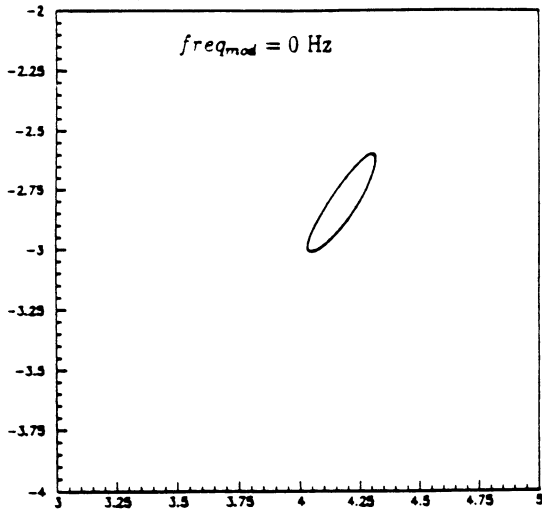


Fig.6a

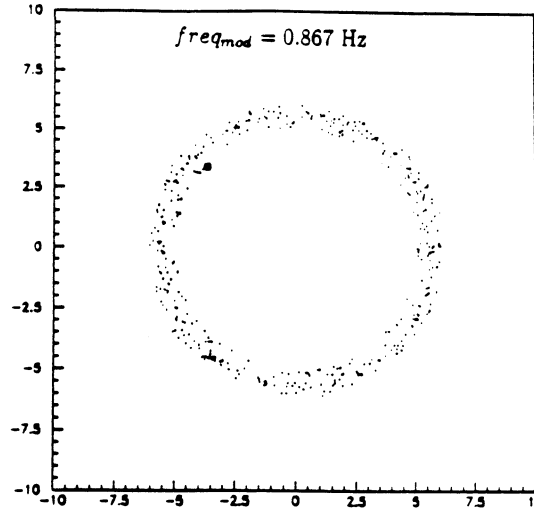


Fig.6b

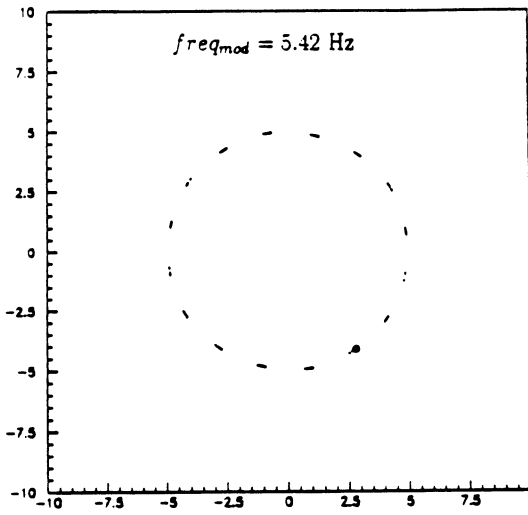


Fig.6c

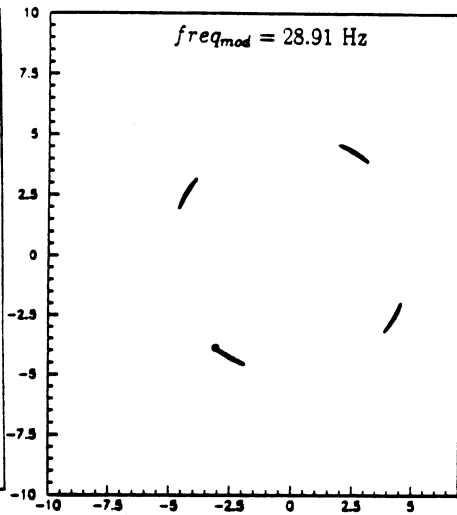


Fig.6d

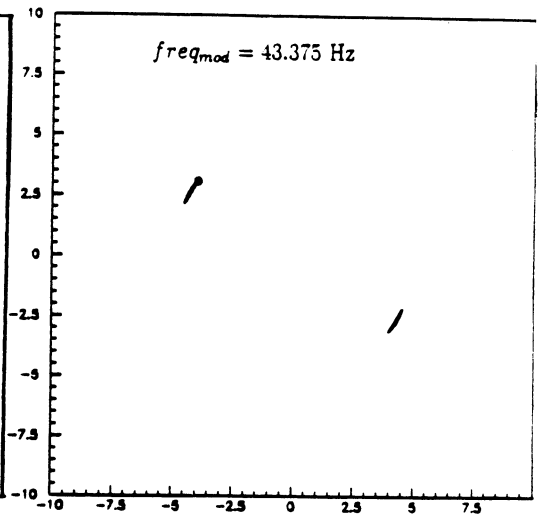


Fig.6e

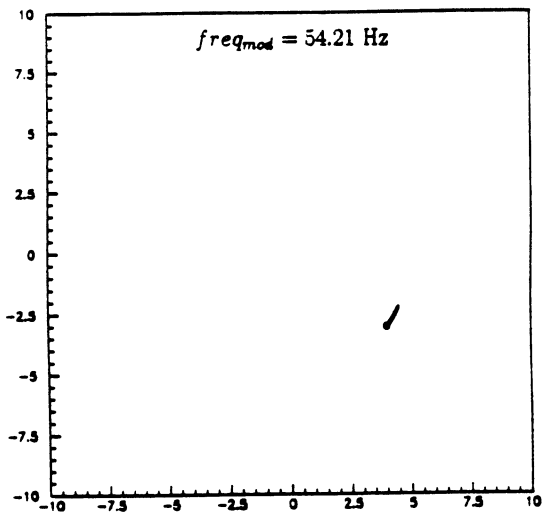


Fig.6f

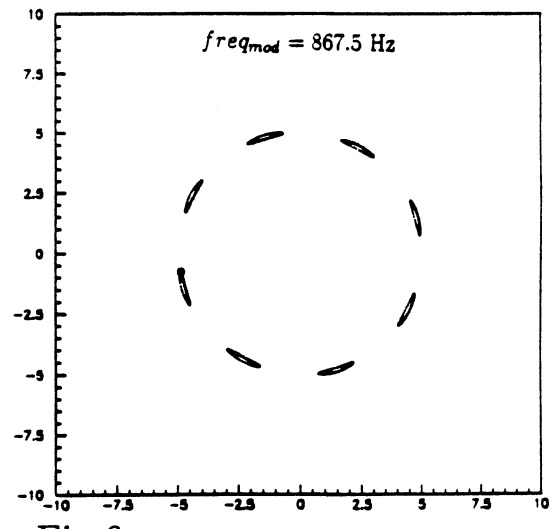


Fig.6g

Fig.6: phase space observations for different tune modulation.

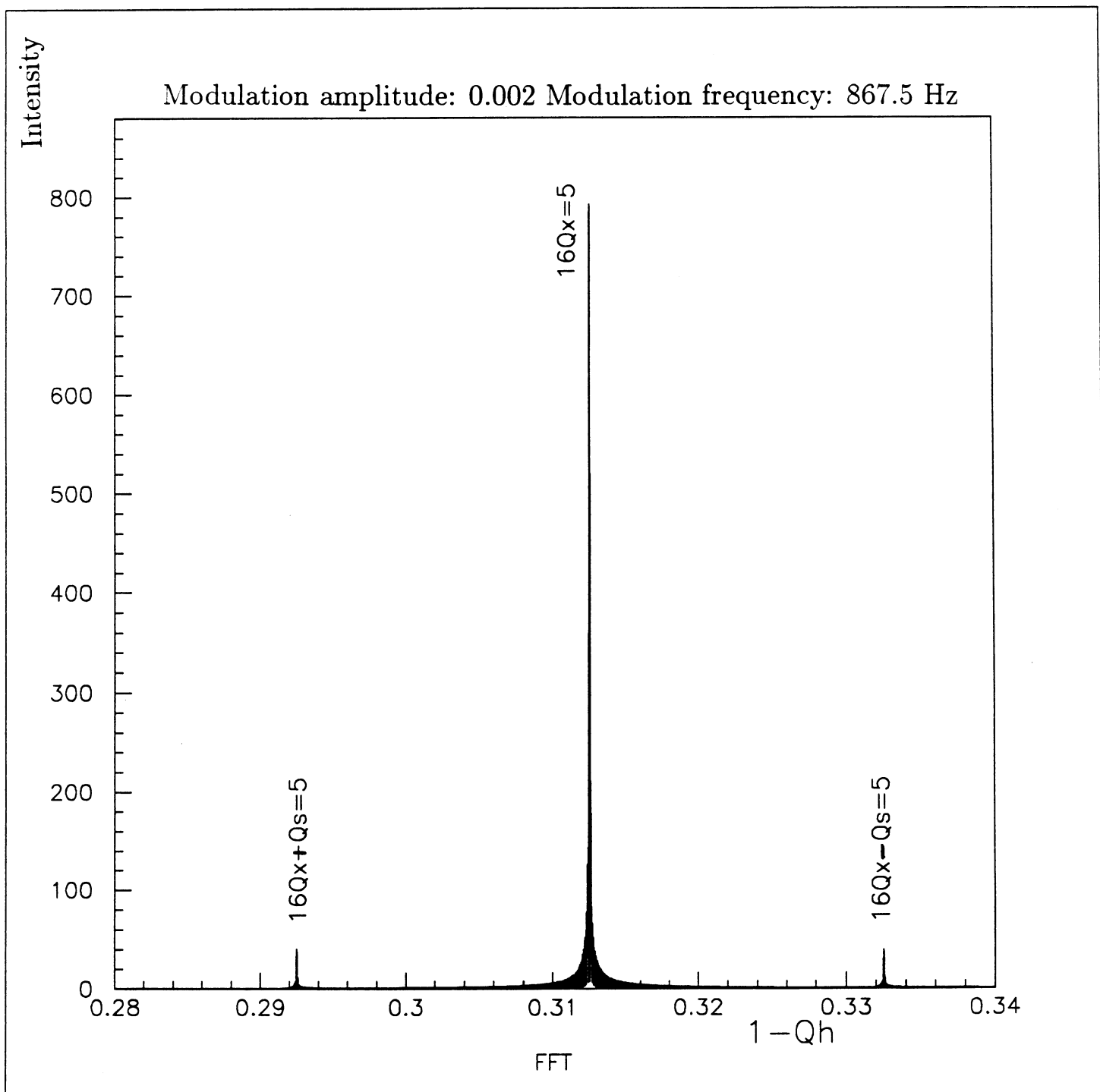


Fig.7: tune spectrum for a modulation frequency of 867 Hz.

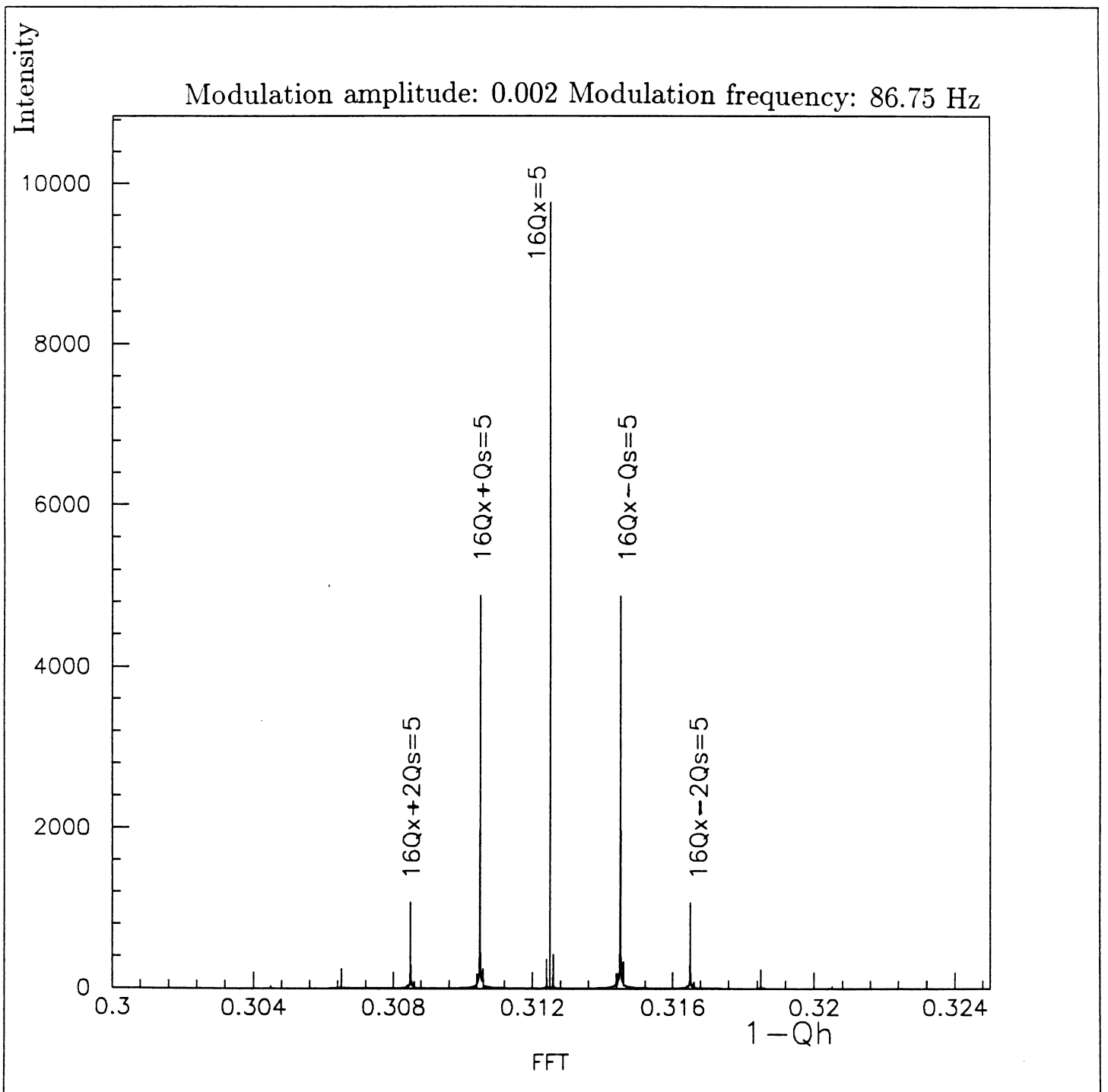


Fig.8: tune spectrum for a modulation frequency of 86.75 Hz.

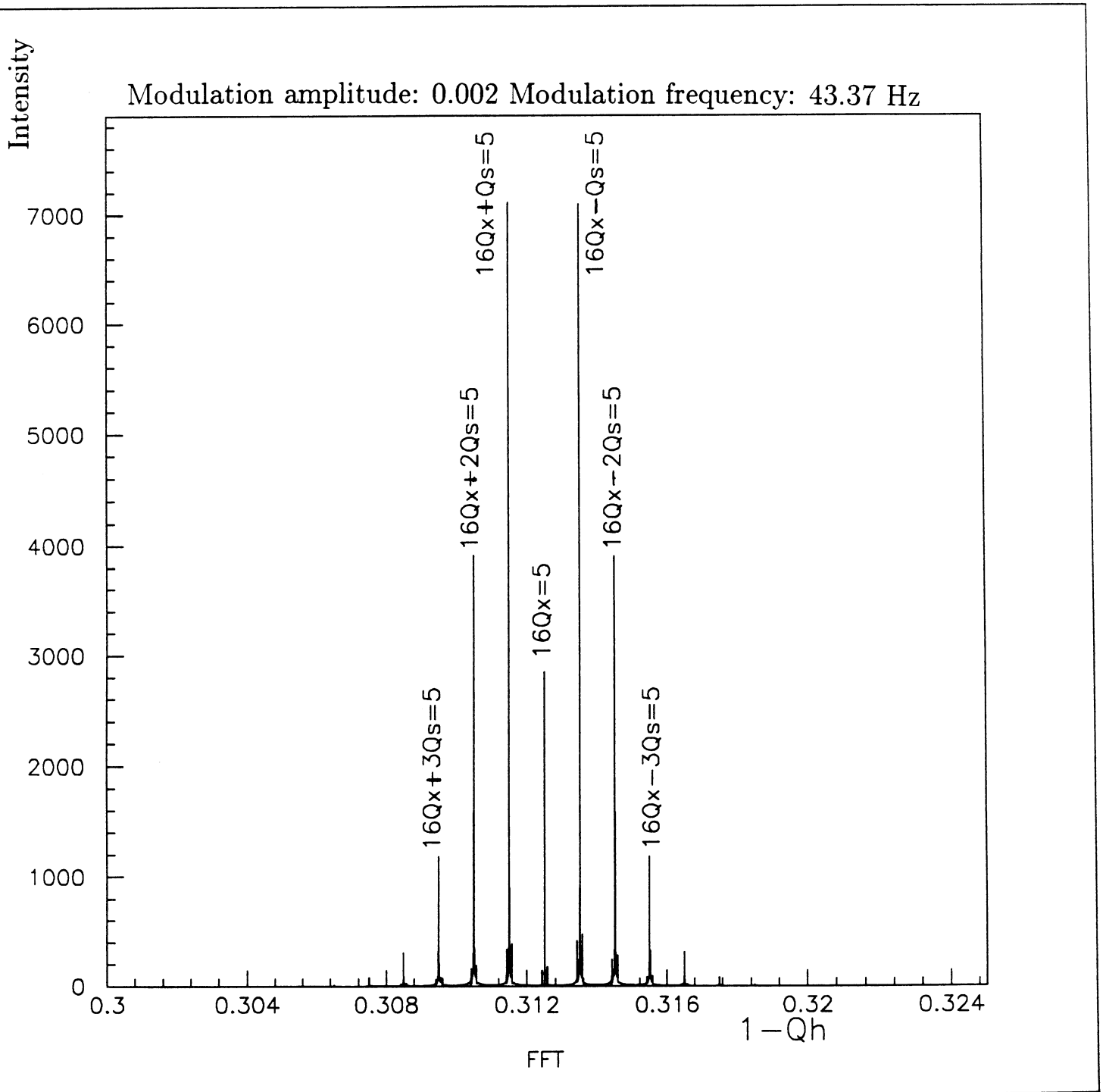


Fig.9: tune spectrum for a modulation frequency of 43.37 Hz.

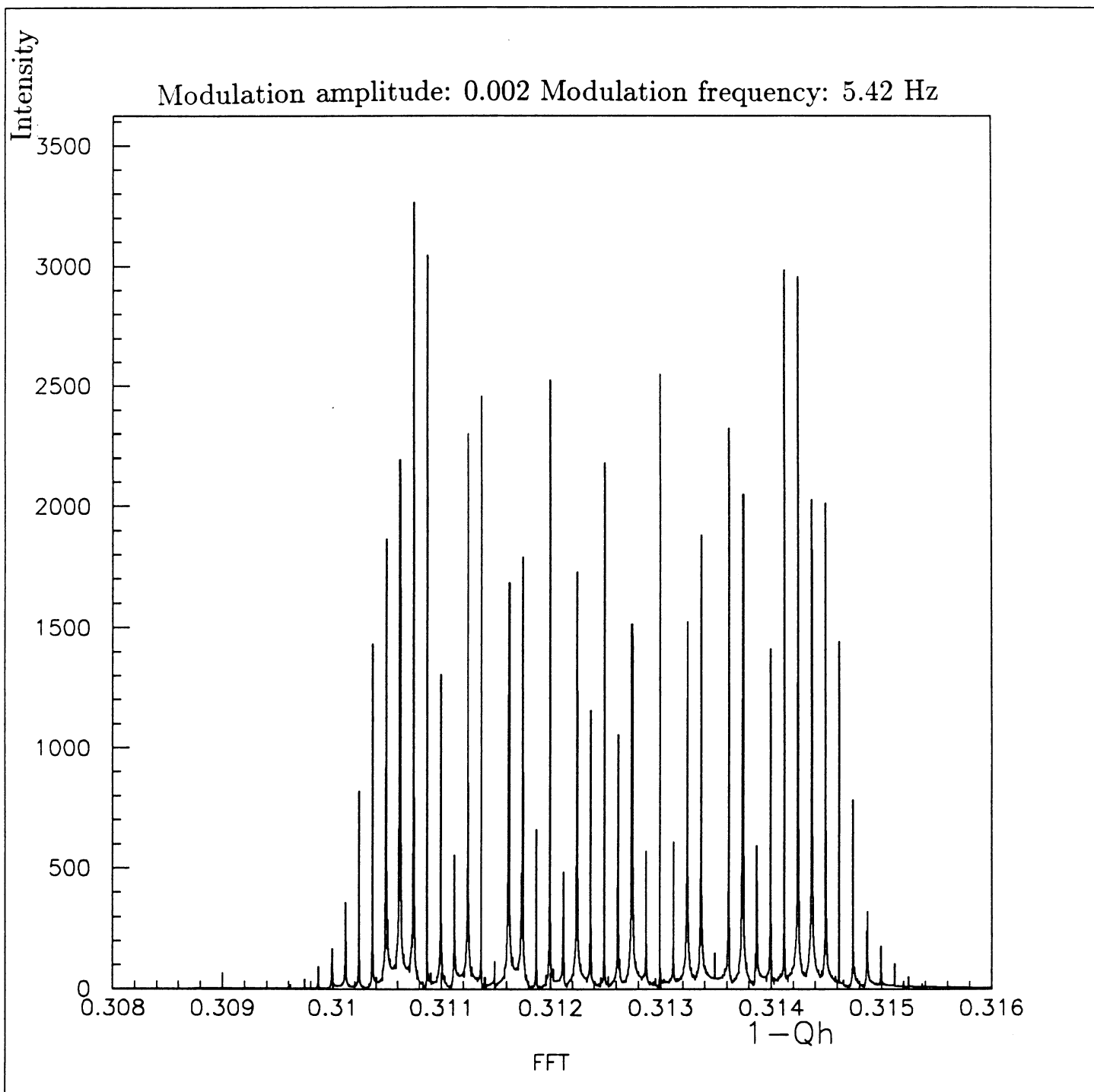


Fig.10: tune spectrum for a modulation frequency of 5.42 Hz.

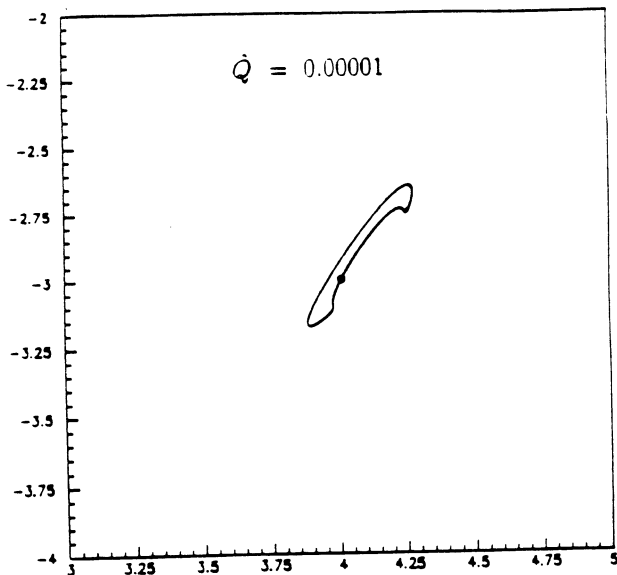


Fig.11a

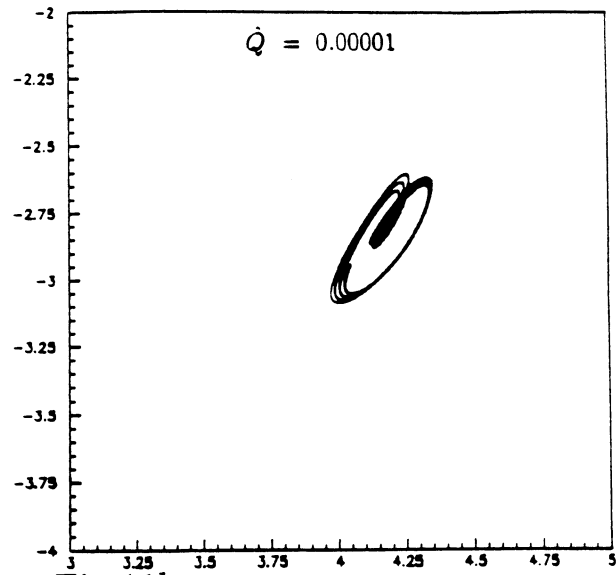


Fig.11b

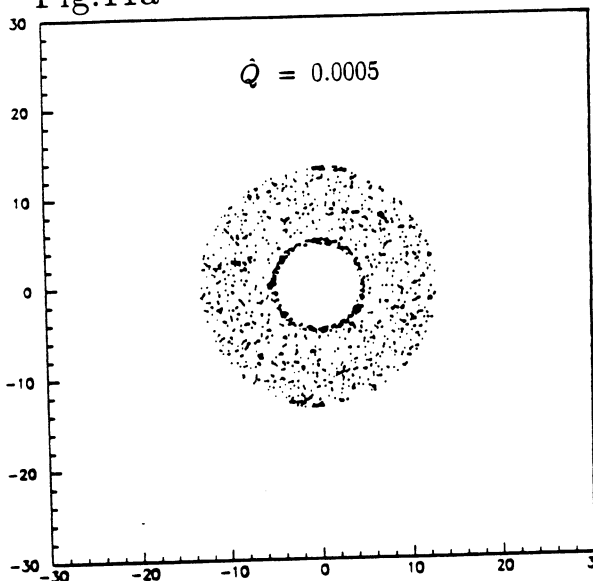


Fig.11c

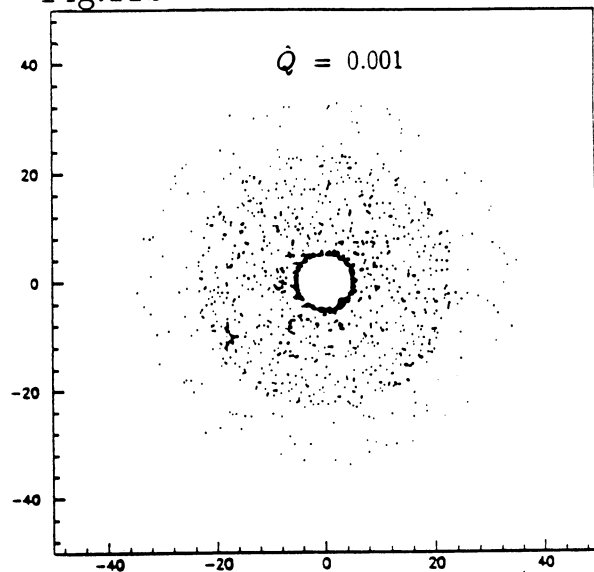


Fig.11d

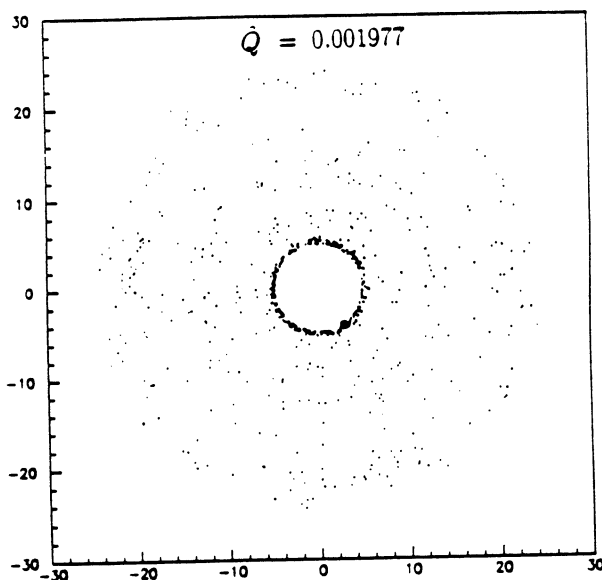


Fig.11e

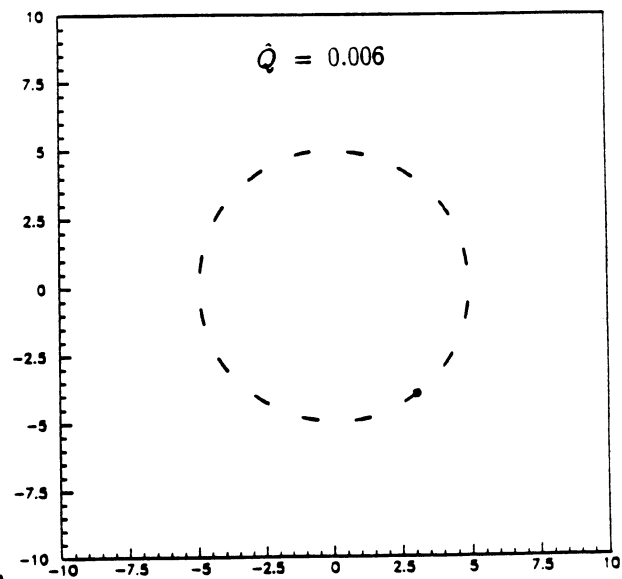


Fig.11f

Fig.11: phase space observations for a modulation amplitude scan.

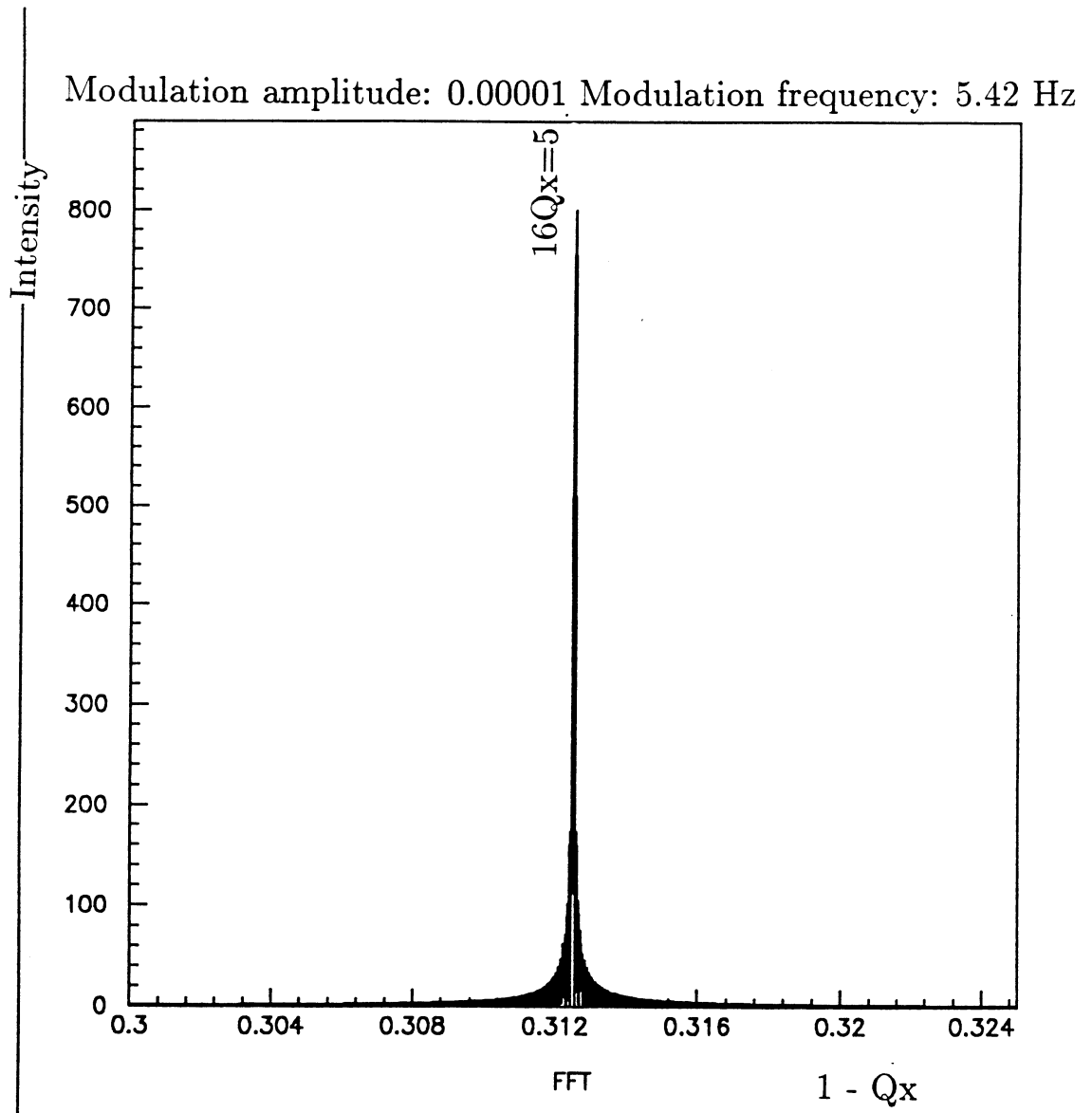


Fig.12: tune spectrum for a modulation amplitude of 0.00001.

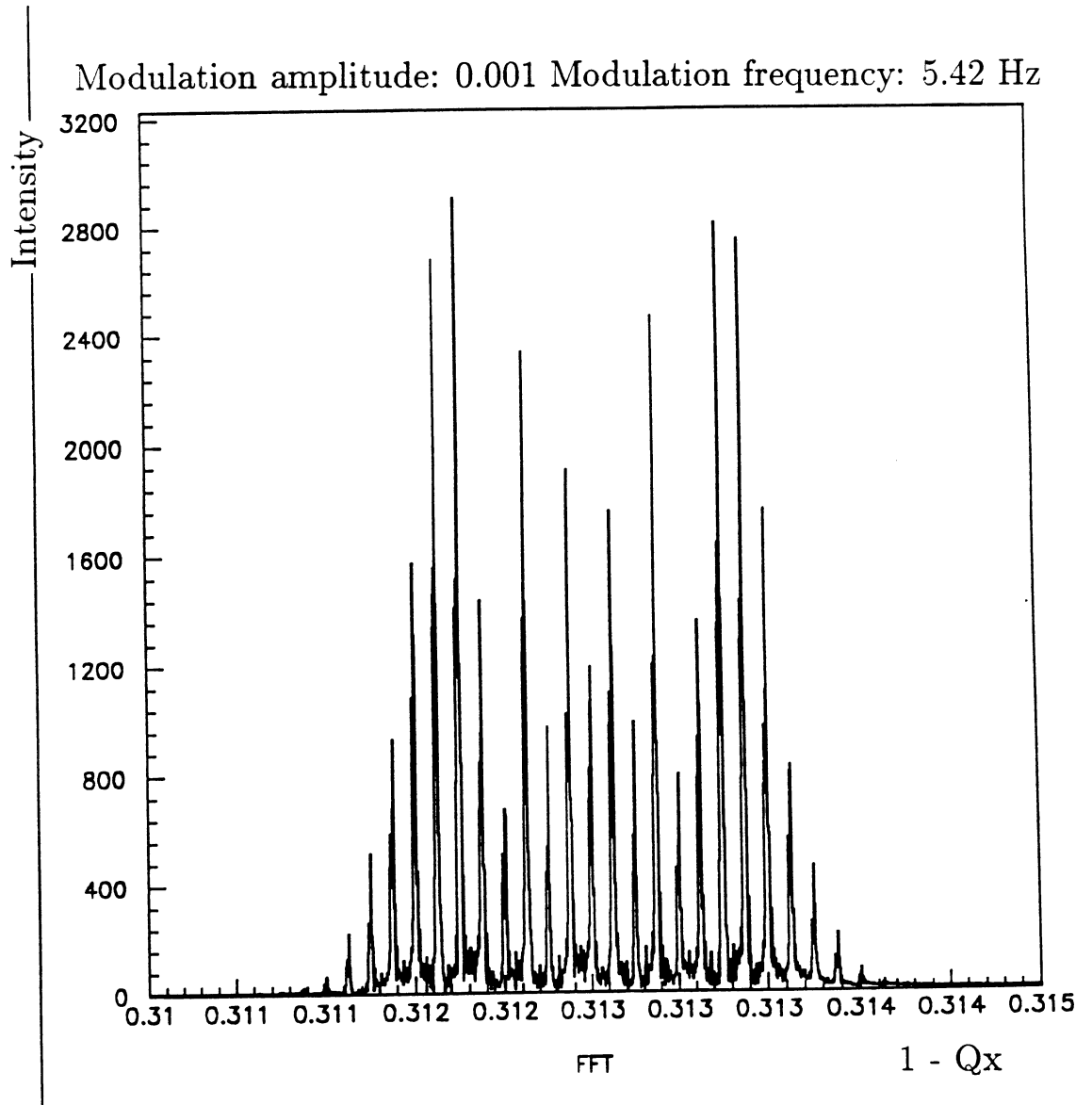


Fig.13: tune spectrum for a modulation amplitude of 0.001

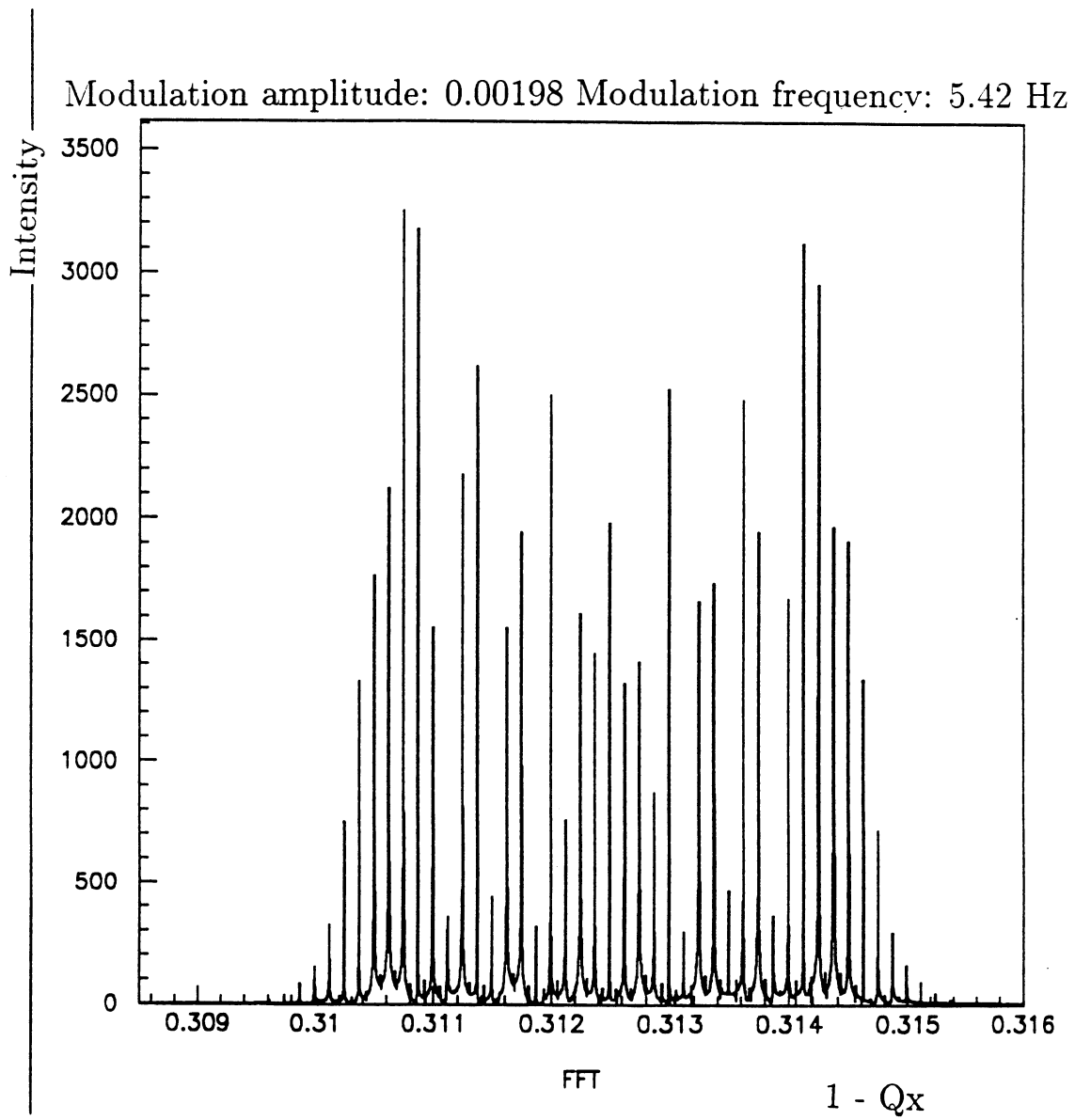


Fig.14: tune spectrum for a modulation amplitude of 0.00198.

Modulation amplitude: 0.00001 Modulation frequency: 86.75 Hz

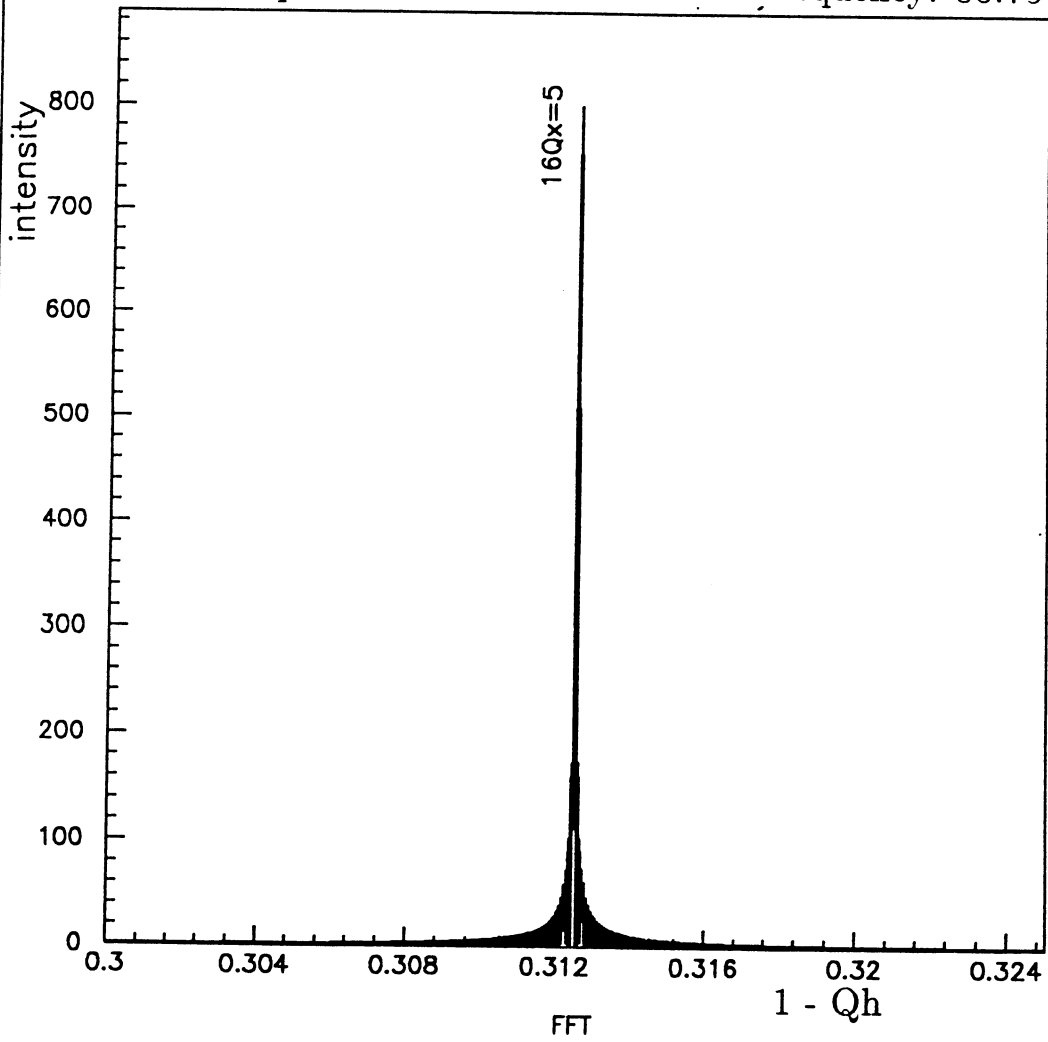


Fig.15: tune spectrum for a modulation amplitude of 0.00001.

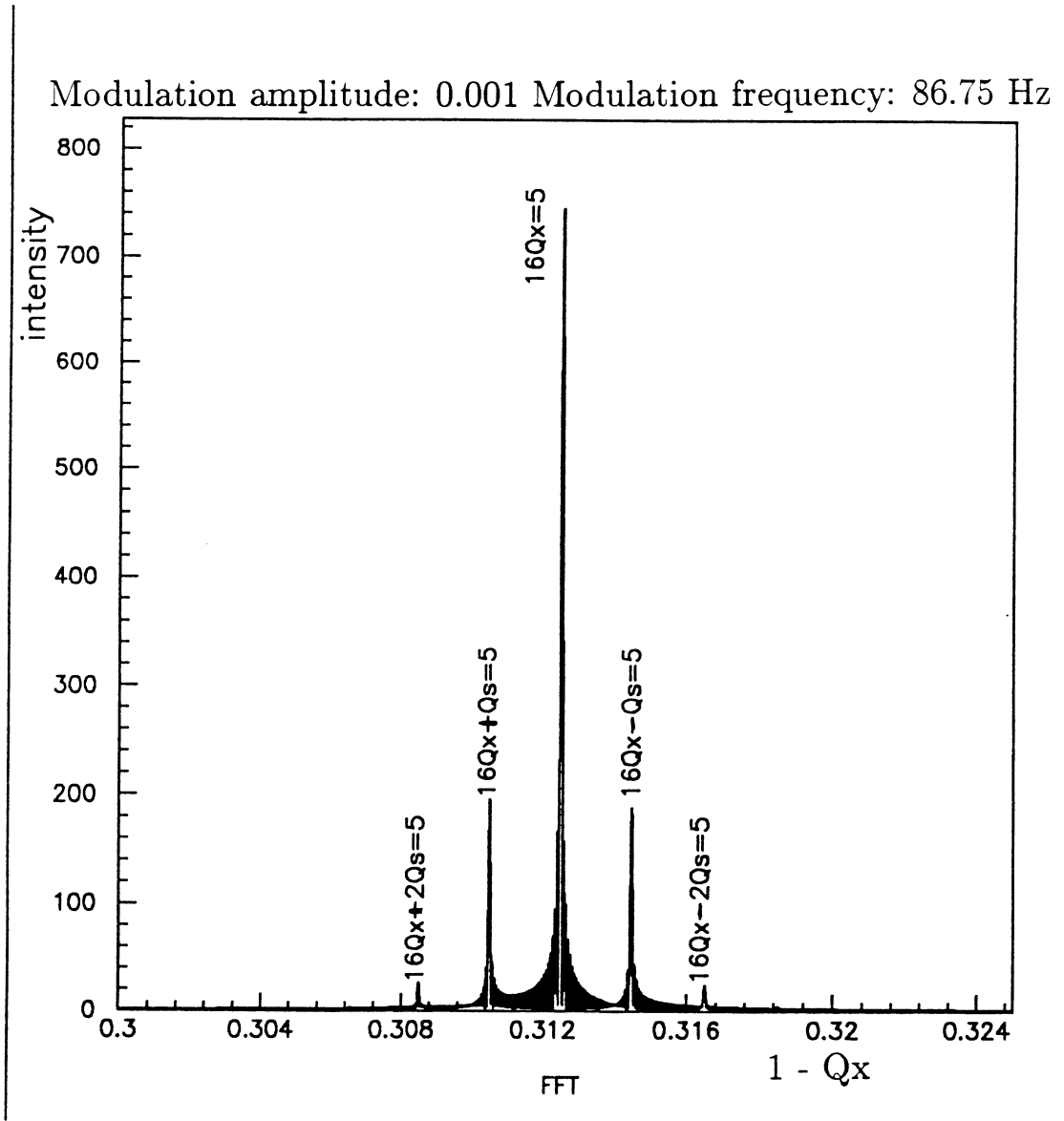


Fig.16: tune spectrum for a modulation amplitude of 0.001.

Modulation amplitude: 0.003 Modulation frequency: 86.75 Hz

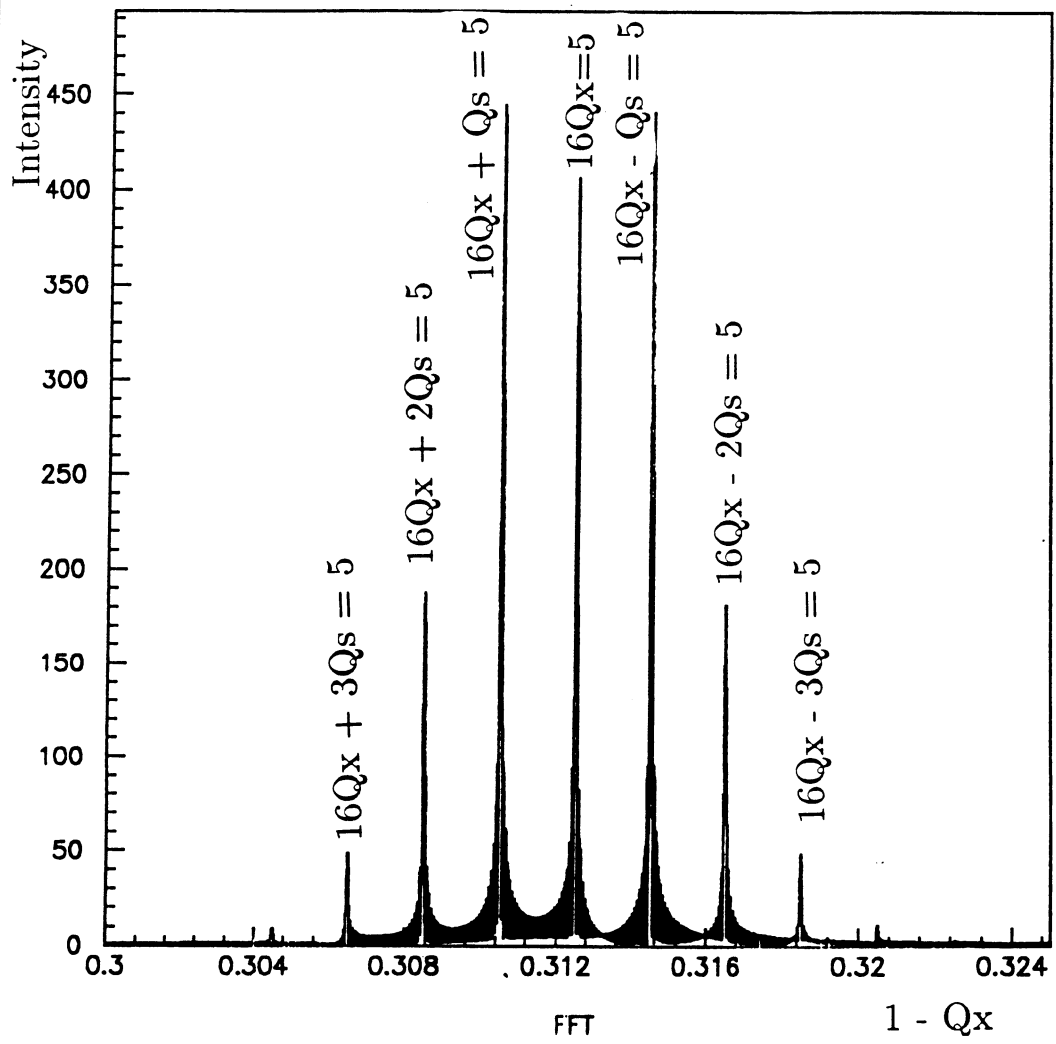


Fig.17: tune spectrum for a modulation amplitude of 0.003.

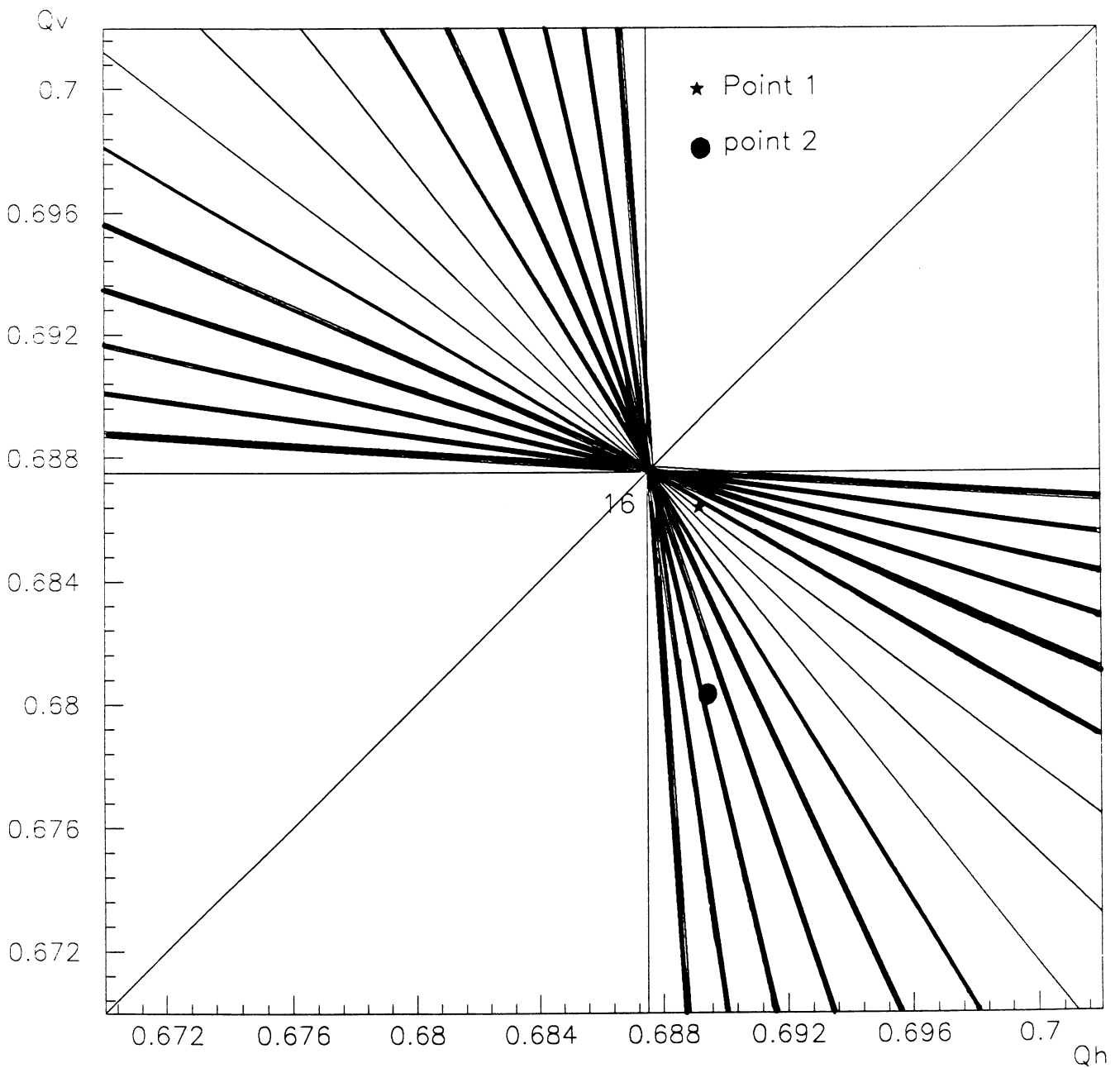


Fig.18: working points for the two dimensional tracking.